Development of Chimeric Lysins to Elucidate the Utility of Sortase Directed Enzybiotics

Robert Newman

MSc by Research (Chemistry)

Acknowledgments

I would first like to thank my supervisor Professor Neil Thomas for all the help and advice he has given me throughout this project. Not only did Professor Thomas give me the research question but his input has also been particularly helpful in refining the direction I approached it in. Importantly, I would also like to thank Professor Thomas for his procurement of funding for the project, and the opportunity to work within the Neil Thomas group.

I would like to thank Dr David Harvey for his assistance with the design and logistics of the project. Dr Harvey was a great sounding board for scrutinizing my thinking and for offering alternatives. Likewise, I wish to thank all members of both the Neil Thomas and Panos Soultanas group. Throughout this year their willingness to share their experience and expertise with me has been invaluable. I would particularly like to thank Thomas Coekin for his supervision when purifying my proteins, and James Kapp for his being a pleasure to both supervise and work alongside. I also wish to especially thank Lenny Ferreira, Isobel Holden, Rowan Earlam, Faadil Fawzy and Dr Alexandra Holland for the countless times I have sought their opinion or assistance. The previous work by Dr Lei Zhang on the Lysostaphin and eGFP constructs was also of great help.

Many thanks also to Robert Markus from the School of Life Sciences Imaging team. Whose assistance with the initial microscopy experimentations unfortunately proved undone by some unruly *E. coli*.

Lastly, I wish to express my immense gratitude to both my friends and family, without whom I likely would have not made it this far. Thank you to my parents for all the many ways they have and continue to support me in all my endeavours.

Abstract

The ability to provide prophylaxis and curative treatment of bacterial infections through the use of antibiotics has become a fundamental pillar of modern medicine. As such, the threat antibiotic resistance poses is of major concern for global health organizations and populations. Pathogenic strains of the commensal Gram-positive bacterium *Staphylococcus aureus* are a common cause of nosocomial infections, with their treatment and management being complicated by the increased prevalence of methicillin and multidrug resistance strains. With few new antibiotics on the horizon and their fate likely to reflect that of their predecessors, it poses the question of what alternatives approaches are available. One such approach is the targeting of the cell wall of *S. aureus* and other Gram-positive bacteria with peptidoglycan digesting enzymes. Exploiting the specificity, modularity and diversity of peptidoglycan hydrolases allows for the selective targeting of the highly conserved peptidoglycan of different Gram-positive species. Key to this approach is the reliable and specific targeting of catalytic domains to the cell wall. As such, this project sought to express and purify eGFP reporter fusions for future use in microscopy and binding assays to evaluate the cell wall anchoring ability of the endogenous Sortase A upon exogenous sort-tagged proteins. To this end we report the successful expression and purification of both SH3b and sort-tagged eGFP fusions despite the occurrence of truncation products stemming from the differing codon usage of its source. An issue also identified with the sequence of Lysostaphin fragments which will be considered in future work. We also report the generation of a DNA construct library, encoding chimeric lysins which will be used in future studies comparing the relative staphylolytic activity of different peptidoglycan hydrolase catalytic domains when fused to either a staphylococcal sort-tag or the cell wall binding domain of Lysostaphin.

Contents:

1. Introduction…… 1

1.1. *Staphylococcus aureus*……1

1.2. Antibiotic Resistance……2

1.3. The Cell Wall……..3

1.4. Peptidoglycan Hydrolases……5

1.5. Peptidoglycan Hydrolase Enzybiotics……10

1.5.1 Chimeric Lysins……11

1.5.2 Lysostaphin Resistance……12

1.5.3. Sortase A……13

1.6. Aims……15

2. Methodology……16

2.1. Chemicals and Reagents……16

2.2. Bacterial Strains and Plasmids……16

2.2.1 Strains……16

2.2.2 Media and Growth Conditions ……16

2.2.3 Plasmids……17

2.3. Transformation of Bacteria……19

2.3.1 Preparation of Competent *E. coli*……19

2.3.2 Transformation of Chemically Competent DH5*α* *E. coli*……20

2.3.3 Transformation of Electrocompetent BL21 (DE3) *E. coli*……20

2.4. Gene Fragments……21

2.5. Manipulations of DNA……21

2.5.1. Isolation of Plasmid DNA……21

2.5.2. Restriction Digest of Plasmid……21

2.5.3. Agarose Gel Electrophoresis……22

2.5.4. DNA Gel Extraction……22

2.5.5. PCR and DNA Cleanup……22

2.6. Primers……23

2.7. Molecular Cloning……24

2.7.1. PCR……24

2.7.2. HiFi Assembly……24

2.7.3. Q5 Site-Directed Mutagenesis……25

2.8. Screening of Recombinant Clones……25

2.8.1. Colony PCR……25

2.8.2. DNA Sequencing……25

2.9. Expression, Purification and Analysis of Recombinant Proteins……26

2.9.1. Small Scale Test Expressions……26

2.9.2. Large Scale Over Expression……27

2.9.3. Purification of Recombinant Protein……28

2.9.4. SDS PAGE……28

2.9.5. Protein Storage……29

2.9.6. Determination of Protein Concentration……29

3. Results and Discussion……..30

3.1. Linearization of pET32a……30

3.2. Amplification of eGFP……32

3.3. Amplification of LSS Fragments……33

3.3.1 Amplification of LSS ……33

3.3.2 Amplification of LSS M23……34

3.4. HiFi Assembly of Gene Constructs……37

3.5. Mutagenesis of LSS Constructs……..43

3.5.1 Restoration of Reading Frames……..43

3.5.2 Insertion of Stop Codon……..45

3.6. Expression of eGFP constructs……46

3.6.1 Test Expression of eGFP-Sort……46

3.6.2 Overexpression of eGFP-Sort……48

3.6.3 Test Expression of eGFP-SH3b……52

3.6.4 Overexpression of eGFP-SH3b……54

4.Conclusion……56

5.Bibliography……59

Abbreviations:

CHAP - Cysteine, Histidine-dependent Amidohydrolases/Peptidases

CWBD – Cell Wall Binding Domain

Cws - Cell wall sorting signal

eGFP – Enhanced Green Fluorescent Protein

GISA - Glycopeptide Insensitive *S. aureus*

INDELs - Insertion or deletions

Lif – Lysostaphin Immunity Factor

LSS – Lysostaphin

LYZ2 - Lysozyme sub family-2

MLS_B - Macrolides, Lincosamides and Streptogramin B

MRSA – Methicillin Resistant *Staphylococcus aureus*

PBP - Penicillin Binding Protein

SDM - Site-Directed Mutagenesis

SpA - Staphylococcal protein A

SrtA - Sortase A

VALs - Virion-Associated Lysins

VISA - Vancomycin Insensitive *Staphylococcus aureus*

VRSA – Vancomycin Resistant *Staphylococcus aureus*

WTAs – Wall Teichoic Acids

1. Introduction

1.1. *Staphylococcus aureus*

Staphylococcus aureus is a commensal bacterium of major clinical importance as an opportunistic human pathogen, causing infections of the blood, pulmonary, bone, epidermis and soft tissues. In developed nations the bacterium is commonly associated with hospital acquired infections, with management representing a significant burden upon modern healthcare systems. This management is complicated by 12-30% of adults being persistent nasal carriers, and up to 69% thought to carry the bacteria intermittently[1]. Recent years have seen the introduction of screening and decolonization programs for patients entering UK hospitals, which along with improved cleaning regimes have reduced rates of nosocomial infections[2]. Despite these successes, an increase in community acquired infections and greater prevalence of methicillin (MRSA), vancomycin (VRSA), or multidrug resistant strains is a major concern to public health globally[3].

1.2. Antibiotic Resistance

Current treatment strategies for *S. aureus* infections can be stratified into a three-tiered antibiotic regimen, based on resistance and severity. Front-line antibiotics are intended to treat low severity non-resistant infections. These include penicillinase-resistant members of the penicillin family such as Flucloxacillin, and first generation cephalosporins (e.g. Cefazolin)[4]. Secondary treatment regimens are employed in severe and resistant infections. In the case of Methicillin resistant infections, a tetracycline may be used independently or in conjunction with Rifamycin or Fusidic acid. Whilst severe infections irrespective of resistance are typically treated with the glycopeptide Vancomycin[5]. The final tier and last resort are Linezolid or Daptomycin which are administered when infections are irresponsive to glycopeptide treatment[5,6]. Although rare, resistance to these last-line of defence antibiotics has been observed[7,8].

The mechanism of action of most antibiotics is the inhibition of pathways involved in key cellular processes such as protein, DNA or cell wall synthesis. As a response, bacteria have evolved a range of resistance mechanisms encoded both chromosomally and within plasmids, the latter of which along with other mobile genetic elements, have facilitated the dissemination of resistance genes between strains and species[9,10]. A major concern for clinicians is the stacking of resistance traits or multidrug resistance. For example, clinical MRSA strains have been isolated that possess genes also conferring resistance to macrolides, lincosamides and streptogramin B (MLS_B)[11]. Whilst the overexpression of *mdeA*, an endogenous efflux pump has been shown to facilitate resistance to several antibiotics[12].

With the incidence of antibiotic resistance increasing globally, the World Health Organization has placed a high priority on the development of new antimicrobials for *S. aureus*[13]. Set against the backdrop of a discovery pipeline that has not produced a novel class of antibiotics since the 80's, and a pharmaceutical industry wary of investing in agents that are likely to either become redundant or held in reserve[14]. It raises the question of whether alternative approaches are available which display greater resilience to the development of resistance.

1.3. The Cell Wall

S. aureus is an archetypal Gram-positive bacterium, with a plasma membrane surrounded by a thick peptidoglycan cell wall. This matrix of peptidoglycan provides the cell with its structural strength, which without would cause the lysis of the cell due to the turgor pressure of the cell contents. It is because of this structural importance that antibiotics such as β-lactams which target cell wall synthesis derive their activity. By inhibiting the transpeptidase activity of Penicillin Binding Proteins (PBP's), these agents not only prevent the assembly of new peptidoglycan chains, but also activate autolysins that digest the existing peptidoglycan[15]. Vancomycin, a glycopeptide class of antibiotic also disrupts cell wall synthesis through the inhibition of transpeptidase activity, however, whilst β-lactams act through the covalent binding of PBP active sites, Vancomycin inhibits transpeptidation by non-covalently binding the D-Alanyl-D-Alanine (D-Ala-D-Ala) substrate of the PBP's making it unavailable for cross-linking[15,16].

The peptidoglycan of *S. aureus* is composed of strands of a hetero-polymer glycan regularly interlinked by stem and cross bridge peptide components. The glycan chain consisting of alternating *N*-acetyl glucosamine (Glc*N*Ac) and *N*-acetylmuramic acid (Mur*N*Ac) residues joined by β1-4 glycosidic bonds is common across bacterial species. In *S. aureus*, stem peptides comprising of L-Ala-D-*iso*-Glu-L-Lys-D-Ala-D-Ala branch off from each Mur*N*Ac residue by way of an amide bond between the carboxyl group of Mur*N*Ac and L-Ala of the stem peptide. Pentaglycine cross-bridges formed between the L-Lys and D-Ala residues of stem peptides from neighbouring glycan chains then interlink the individual chains into a complex matrix. The degree of this cross-linking is very high in *S. aureus,* with most individual glycan strands being relatively short[17-19].

1.4. Peptidoglycan Hydrolases

Peptidoglycan hydrolases (lysins) are a diverse group of enzymes capable of hydrolysing different covalent bonds within the peptidoglycan cell wall of bacteria. Found across the different domains of life, these enzymes can be further grouped based upon their origin and the biological function they perform. In bacteria, peptidoglycan hydrolases perform two distinct functions and as such are divided into two groups. Autolysins act on the cell wall of the bacteria that produce them, where they play an important role as cell wall remodellers involved in cell growth, cell division and biofilm formation[20-22]. Exolysins, alternatively, do not act on the cell wall of the producing bacteria but upon those of competing species. They function to degrade the cell walls of these competitors, inducing cell lysis and therefore provide competitor inhibition[23]. Analogues of these exolysins are found in eukaryotes, where their antibacterial activity forms part of the innate immune system[24]. Two other groups originate in lytic bacteriophage (phage) and are employed at distinct stages of their lifecycle. Virion associated lysins (VALs) facilitate the initial invasion of bacterial cells through the local digestion of the cell wall at the point of attachment[25]. Whereas endolysins facilitate cell lysis of the host and the subsequent release of prophage through the complete digestion of peptidoglycan[26].

Although VALs, endolysins, exolysins and autolysins are broadly unrelated with little sequence homology between the classes, they do often display a common modular structure. With individual modules that represent distinct catalytic and cell wall binding domains (CWBD's) (see Figure 1). A primary exception are endolysins from Gram-negative infecting phage which are predominantly single-domain globular proteins[27,28].

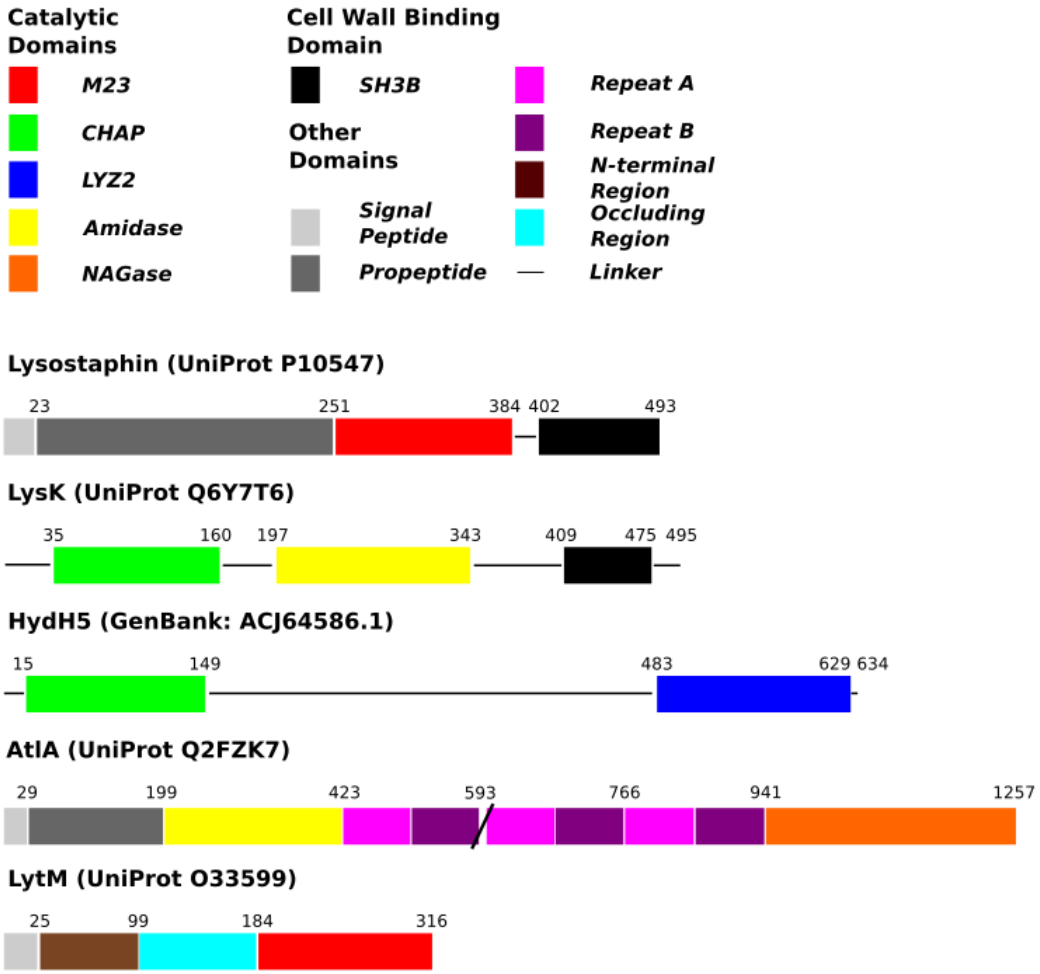


Figure 1. Schematic representation of the modular structures found in peptidoglycan hydrolases with specific activity for the peptidoglycan of *S. aureus*. Lysostaphin represents an exolysin from *S. simulans*, LysK and HydH5 an endolysins and VAL from *S. aureus* infecting phage respectively, while the autolysins AtlA and LytM originate from *S. aureus*. Multiple catalytic domains may be present as seen in LysK and AtlA although both may not actually display catalytic activity, as displayed by the Amidase domain of LysK. The two catalytic domains of AtlA act independently as they are post-translationally cleaved between the first and second repeat regions. Numbers represent the amino acid position of domain barriers and protein length[29-33].

Catalytic domains and by way of their possession; peptidoglycan hydrolases, are classified by their enzymatic activities. These activities belong to three over-arching classes: glycosidases, amidases and endopeptidases. Glycosidases can be further divided into *N*-acetylmuramoyl-β-D-muramidases (muramidases) and *N*-acetyl-β-D-glucosaminidases (glucosaminidases) based on which bond between the Glc*NA*c and Mur*N*Ac residues of the glycan backbone they cleave. Muramidases cleave the *N*-acetylmuramoyl-β-1,4-*N*-acetylglucosamine bond, and glucosaminidases cleave the alternative *N*-acetylglucosaminyl-β-1,4-*N*-acetylmuramine bond. Amidases cleave the amide bond between the *N*-acetylmuramoyl sugar and the first amino acid of the stem peptide. In *S. aureus* this amino acid is L-alanine, making these *N*-acetylmuramoyl-L-alanine amidases. Endopeptidases encompass the cleavage of any peptide bonds within the stem or cross-linker peptides. Although the activity of individual endopeptidases are restricted to specific residues. It is worth noting that another group of catalytic domains found in lytic proteins are the transglycosylases, which like glycosidases cleave the β-1,4-glycosidic bond. However, because they employ a different mechanism, involving the formation of 1,6-*anhydromuramyl* residues they are not peptidoglycan 'hydrolases'[34].

Lysostaphin (LSS) is an staphylolytic exolysin secreted by the *Staphylococcus simulans* biovar *staphylolyticus*[35]. The mature LSS protein comprises of an N-terminal M23-family zinc metalloendopeptidase catalytic domain, joined to a C-terminal SH3b CWBD by a highly flexible linker region[36] (see Figure 1). This M23 domain hydrolyses glycyl-glycl bonds at the 2-3 and 3-4 positions within pentaglycine crossbridges[37] (see Figure 2).

Another staphylolytic protein with endopeptidase activity is LysK, an endolysin from the staphylococcal phage K[38]. Interestingly, although LysK possesses both an N-terminal CHAP domain and a central amidase-2 domain (see Figure 1), it appears the staphylolytic activity is reliant on the endopeptidase action of the CHAP (Cysteine, Histidine-dependent Amidohydrolases/Peptidases) domain[29,38], cleaving the alanyl-glycyl bond between the stem peptide and pentaglycine crossbridge (see Figure 2).

HydH5 is a VAL from the *S. aureus* bacteriophage vB_SauS-phiIPLA88. Like LysK it also contains two active catalytic domains; an N-terminal CHAP domain and a C-terminal Lysozyme sub family-2 (LYZ2) domain[39] (see Figure 1). The endopeptidase activity of the CHAP domain cleaves glycyl-glycyl bonds along the cross bridge with a preference for the 3,4 position, while the LYZ2 domain shows muramidase activity (see Figure 2)[26,39]. Unlike LysK and LSS, HydH5 lacks a CWBD because HydH5; thought to be located within the phage baseplate, is localized to the cell wall during phage docking.

AtlA is the major autolysin of *S. aureus* playing an essential role in cell division [40]. AtlA is expressed as a precursor protein that is post-translationally cleaved at an interlinking repeat region to produce active amidase (AmiA) and glucosaminidase (NAGase) catalytic domains[41] (see Figure 1). These mature proteins are then directed to the septal ring where they play a role in septal division and peptidoglycan remodelling during cell division. This localization is facilitated by the exclusory behaviour of wall teichoic acids (WTAs) found on mature peptidoglycan towards the peptidoglycan binding repeat domains[42].

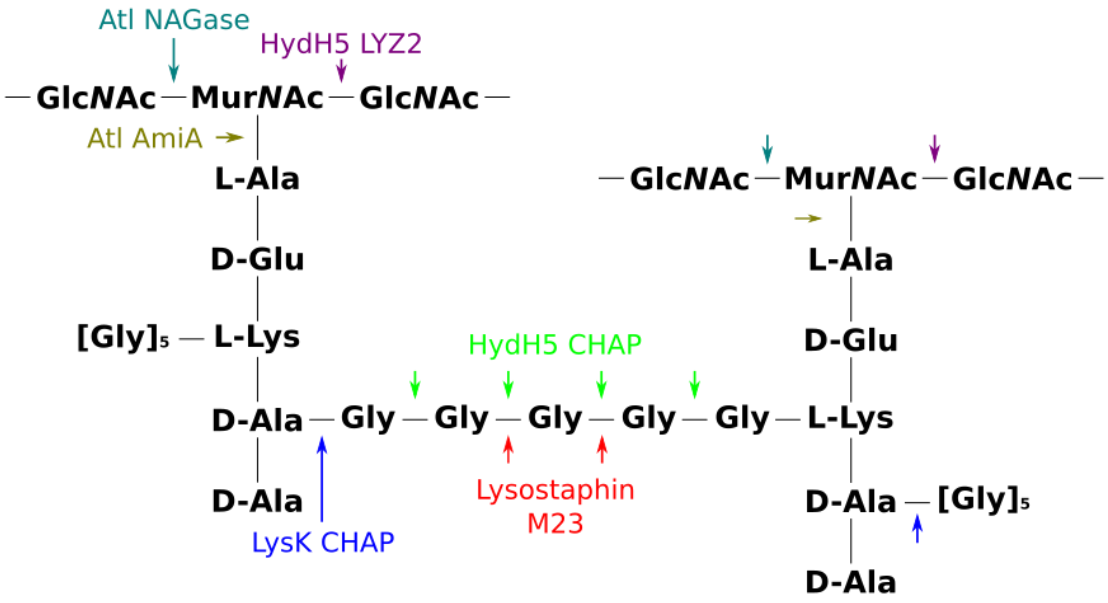


Figure 2. Organisation of *S. aureus* peptidoglycan and cleavage sites of catalytic domains of interest. LSS M23, LysK CHAP and HydH5 endopeptidase activities are specific for specific positions in the pentaglycine bridge. Atl amidase (AmiA) domain cleaves the amide bond linking the stem peptide from L-alanine to the *N*-acetylmuramic acid of the glycan backbone. Atl *N*AGase and HydH5 LYZ2 domains cleave glycosidic bonds between the Glc*N*Ac and Mur*N*Ac residues of the glycan backbone via glucosaminidase and muramidase activity respectively[29,37,39,41].

1.5. Peptidoglycan Hydrolase Enzybiotics

Although the term 'Enzybiotic' is often used synonymously with that of 'peptidoglycan hydrolase', the former could comprise any enzyme used as an antibiotic whilst the later merely describes a group of proteins with broadly similar activity and no inherent therapeutic use. The idea of using peptidoglycan hydrolases as enzybiotics stems from the use of phage to treat bacterial infections. Whilst the discovery and rapid adoption of antibiotics throughout the 20th century meant that the field of phage therapy has remained on the fringes of modern medicine. However, the growing concern over rising antibiotic resistance has renewed interest in phage. Despite promising effectiveness, specificity and low immunogenicity; concerns over scalability, safety, resistance, and regulatory barriers pose significant obstacles to the mainstream adoption of phage therapy[43-45]. The heterogenous nature of phage and their ability to specifically target different strains of bacteria is perhaps the primary reason for these concerns. Presenting a challenge to a pharmaceutical regulation system that is designed for the assessment of clearly formulated medicines rather than the formulative tailoring of which phage therapy requires.

Isolated peptidoglycan hydrolases however pose an attractive workaround. With many phage endolysins and VALs maintaining their lytic activity separate from their parent virions, these enzymes are being explored as potential enzybiotics[46-49]. Additionally, as purified proteins they can be administered independently, in combination or along with antibiotics[50]. Two such therapies, CF-301 and SAL200 (N- Rephasin®) are now in phase II clinical trials for treatment of persistent *S. aureus* bacteraemia in combination with standard antibiotic treatment[51,52].

1.5.1 Chimeric Lysins

The modular nature of peptidoglycan hydrolases allows for the detachment and rationalization of individual catalytic and CWBD functions. This ability allows for the engineering of novel chimeric lysin enzybiotics with improved binding affinity, altered targeting, and improved bactericidal activity[53,54]. Two such enzybiotics have entered clinical trials: P128 for MRSA nasal decolonization and Staphefekt SA.100; which is already available for cosmetic use, is undergoing trials for atopic dermatitis[55-57]. These and many other chimeric lysins that are being studied for anti-staphylococcal activity include LSS domains[56,58]. LSS itself has been investigated as a potential therapeutic for *S. aureus* infections; in particular those displaying antibiotic resistance[59-63], and has displayed anti-biofilm properties[64,65].

The LSS SH3b domain is commonly selected for fusion to different catalytic domains because of its high affinity for the peptidoglycan of *S. aureus* and *Staphylococcus epidermis*[66]. Although the exact mechanism of its binding has yet to be fully elucidated, co-precipitation and crystallization studies suggest the domain shows affinity for the stem peptide, with a pentaglycine binding groove playing a modulatory roll[67,68]. The fusion of the LSS SH3b domain to various catalytic domains has demonstrated its ability to expand and increase lytic activity[30,69-71], including the M23 catalytic domain of the *S. aureus* autolysin LytM which displays little activity in its original protein due an C-terminal region that occludes the domains active site[31,72] (see Figure 1).

1.5.2 Lysostaphin Resistance

One of the motivations for studying such fusions is to address the issue of LSS resistance. Although rare, lysostaphin resistance is most commonly associated with mutations within the *femABX* operon[73]. The *femA* and *femB* genes encode aminoacyltransferases responsible for the incorporation of glycines at the 2,3 and 3,4 positions respectively[74]. The knockout of either *femA* or both results in the shortening of crossbridges to a single monoglycine, interfering with SH3b binding and removing the M23 cleave site[75,76]. These mutations do however result in reduced fitness, with mutant MRSA strains displaying: slower growth, increased temperature sensitivity, reduced virulence, and increased β-lactam susceptibility[77,78].

Another mechanism of resistance is the substitution with non-glycine residues. This can be observed in the lysostaphin producing *S. simulans*, which possesses the Lif (lysostaphin immunity factor) gene. This gene encodes a *FemABX*-like aminoacyltransferase which confers immunity through the incorporation of serine residues at positions 3 and 5 within the crossbridge[35,73,79]. Incorporation of serine not only disrupts the cleavage site of the M23 domain, but also likely impedes the entry of the cross-bridge into the binding groove of SH3b, inhibiting the domains binding[68]. It is however worth mentioning that such residue substitutions are uncommon in *S. aureus* and horizontal transfer of the Lif gene has not been observed.

1.5.3. Sortase A

Whilst mutations arise that alter peptidoglycan composition, the ability to use different catalytic domains that either target residues with more stringent conservation or show greater substrate flexibility provides a promising barrier to the development of resistance. These mutations do however pose an issue for the choice of CWBD[68]. Unlike catalytic domains, currently there is not the diversity or understanding of alternative CWBD's to replace the LSS SH3b domain when targeting *S. aureus*[80-82]. Potential alternatives to a CWBD could include domains from other peptidoglycan binding proteins, or the generation of peptidoglycan specific epitope binding single chain antibodies / antibody mimetics. Another alternative is to utilize the endogenous cellular machinery *S. aureus* uses for anchoring proteins to its cell wall (see Figure 3).

The Sortase family of cysteine transpeptidases are responsible for the covalent attachment of wall associated proteins by Gram positive species. In *S. aureus*, Sortase A (SrtA) is responsible for the attachment of LPXTG motif containing surface proteins. These proteins make up the majority of surface proteins and have a number of important roles in pathogenesis, making the function of SrtA integral to virulence[83]. It is because of its importance to pathogenesis and high degree of conservation between Gram-positive species, that SrtA has become a target for anti-infective drug discovery[84]. With SrtA inhibitors shown to impair adhesion and biofilm formation *in vitro*[85,86], and be to protective during murine mastitis and bacteraemia models of infection[87,88].

SrtA a plasma membrane-bound protein consists of an N-terminal membrane-spanning domain and C-terminal extracellular catalytic domain[89]. The catalytic domain catalyzes the cleavage of LPXTG motifs between the threonine and glycine, and the formation of a peptide bond between the free carboxyl-group of threonine and the free amine-group of the terminal glycine of lipid II[90,91] (see Figure 3). The low substrate specificity of SrtA has allowed its exploitation in a range of applications[92,93], and makes it suitable for incorporating heterologous proteins containing LPXTG motifs.

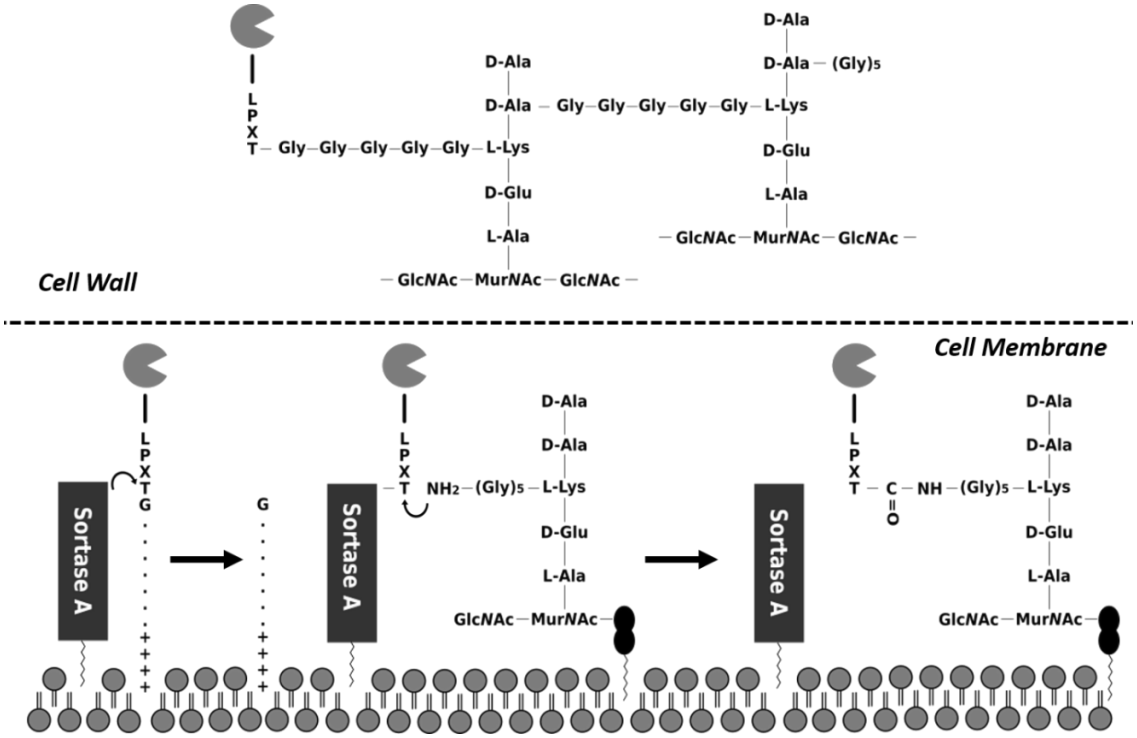


Figure 3. Anchoring of a chimeric lysin to nascent peptidoglycan by Sortase A. Anchoring is initiated at the cell membrane where Sortase A cleaves the LPXTG motif between the threonine and glycine, creating a Sortase A-lysin intermediate and releasing the cell wall sorting signal. Sortase A then recognizes its second substrate Lipid II, catalyzing the nucleophilic attack of the thioacyl bond by the N-terminal glycine of the pentaglycine cross-bridge. Further transpeptidation and glycosylation reactions then assemble these peptidoglycan disaccharide monomers into the cross-linked chains that comprise the cell wall[90,91].

Protein A is an important virulence factor, facilitating host immune evasion through the binding immunoglobulins and cross-linking B cell receptors[94,95]. Like all SrtA anchored proteins its LPXTG motif is contained within a larger C-terminal cell wall sorting signal (Cws)[96]. This region consists of the LPXTG motif, a hydrophobic domain and a positively charged tail. Mutagenesis studies have shown that deletion of anyone of these regions results in abrogated Protein A anchoring, and have also demonstrated that fusion of the Protein A Cws is sufficient for the anchoring of heterologous proteins[96]. It has also been shown that exogenous peptides with either LPXTG motif or the larger Cws can be incorporated by endogenous SrtA, with the Cws increasing the efficiency[97,98]. As such, the Cws of Protein A has been chosen as a fusion partner to establish the feasibility of anchoring peptidoglycan hydrolase catalytic domains to the staphylococcal cell wall via endogenous SrtA.

1.6. Aims

This project aims to:

- Amplify LSS and eGFP gene fragments for construct assembly.
- Generate a construct library encoding peptidoglycan hydrolase catalytic domains fused to either the LSS SH3b CWBD or Protein A Cws.
- Generate constructs for the expression of eGFP with and without C-terminal fusion of the LSS SH3b CWBD or Cws of Protein A.
- Optimise the expression and purification of eGFP and eGFP fusion proteins.

2. Methodology

2.1. Chemicals and Reagents

All chemicals or reagents where unstated were supplied by Sigma-Aldrich.

2.2. Bacterial Strains and Plasmids

2.2.1 Strains

Plasmids were maintained within the *recA* recombinase and *endA* endonuclease deficient *DH5α* (New England Biolabs) *Escherichia coli* strain. Whilst recombinant protein was expressed in the Lon and OmpT protease deficient BL21 (DE3) (New England Biolabs) expression strain. Strains were stored at -80 ^{o}C in 25% (v/v) glycerol supplemented media.

2.2.2 Media and Growth Conditions

Both *E. coli* strains were grown in LB-Miller media (Sigma) or on LB-Miller agar plates and were supplemented with ampicillin (100 µg/mL) for selection of plasmid maintaining clones. Liquid DH5*α* cultures were shaken at 180 rpm at 37 ^{o}C overnight (12-16 hours), and agar plate cultures also incubated at 37 ^{o}C overnight. Liquid BL21 (DE3) cultures varied in their growth conditions due to optimization for protein expression.

2.2.3 Plasmids

Gene constructs were assembled directly into the multiple cloning region of the pET32a expression vector (Novagen) displayed in Figures 4a and 4b.

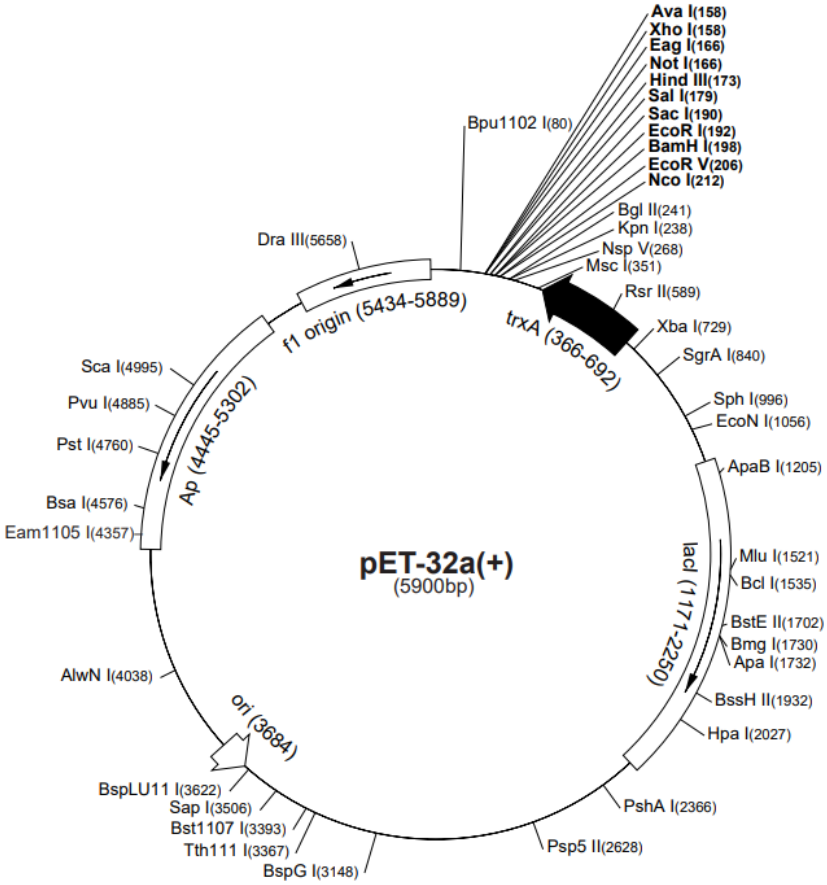


Figure 4a. Plasmid map of pET-32a[99].

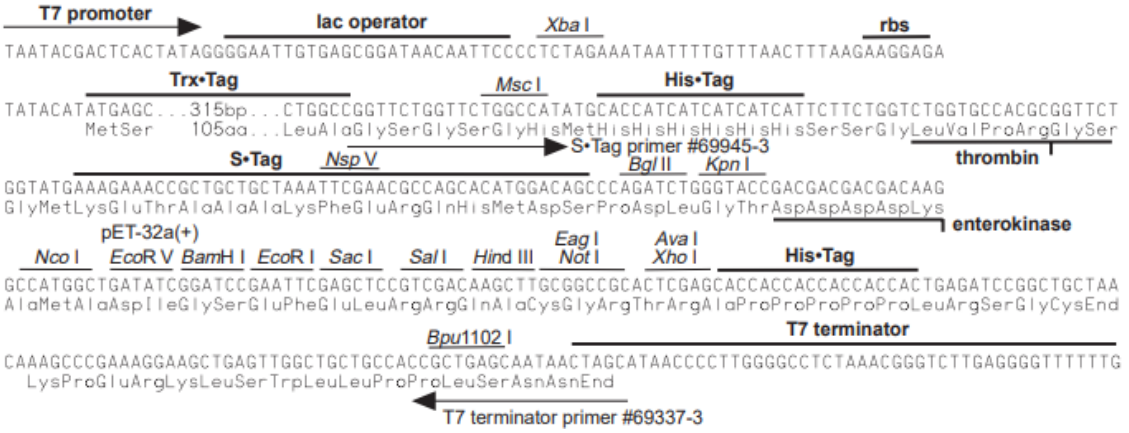


Figure 4b. Cloning region of pET32a[99]. Gene constructs were cloned into the *Nco*I site and transcribed by T7 polymerase under regulation of the lac repressor system. The resulting translated proteins contained a N-terminal region comprising of a Thioredoxin solubility tag, Ni-binding His Affinity Tag for purification, a Thrombin cleavage motif, S Affinity Tag, Enterokinase cleavage motif located proximally to the N-terminus of the desired protein. Stop codons were added to the end of inserted sequences so to occlude translation of the C-terminal His-Tag.

Previous work by Dr Lei Zhang in the Thomas group had cloned LSS and eGFP into the pET30a (Invitrogen) and pJ414 (DNA 2.0 / ATUM) expression plasmids, respectively. The coding sequence of LSS had been inserted along with a C-terminal truncation of the staphylococcal Protein A (SpA). The resulting translated protein would therefore comprise of an LSS-SpA fusion with N-terminal His and S-tags. Additional thrombin and enterokinase cleavage sites were located to remove the N-terminal His-Tag and C-terminal SpA fragment, respectively. Similarly, eGFP was cloned into pJ414 so to be expressed with a C-terminal His-Tag, which was designed to be cleaved upon processing of an interspacing sort-Tag. The two plasmids pET30a-LSS and pJ414-eGFP provided templates for the amplification of LSS and eGFP fragments.

2.3. Transformation of Bacteria

2.3.1 Preparation of Competent *E. coli*

Calcium chloride competent DH5*α* cells were prepared and divided into aliquots for storage as follows: 10 mL of LB was inoculated with cells from a thawed glycerol stock of DH5*α* and grown overnight. Another 10 mL of sterile LB was inoculated with 100 µL of the overnight culture and left to grow (37 ^{o}C, 180 rpm) until reaching an OD_{595} of approximately 0.3. Cells were then pelleted by centrifuge (Heraeus Biofuge Prime R) at 3000 *g* for 10 minutes at 4 ^{o}C, the supernatant discarded and resuspended in 5 mL of ice cold 50 mM $CaCl_2$. This step was repeated, and the resulting cell pellet was resuspended in 40 mM $CaCl_2$, 10% (v/v) glycerol. Finally, 50 µL aliquots of cells were snap frozen with liquid nitrogen and stored at -80 ^{o}C.

Electrocompetent BL21 (DE3) cells were prepared and divided into aliquots for storage as follows: BL21 (DE3) cells from a thawed glycerol stock were streaked onto an antibiotic-free agar plate and incubated overnight. A single colony from the plate was then used to inoculate 10 mL of sterile LB and grown overnight. This 10 mL starting culture was then used to inoculate 500 mL of LB and grown (37 ^{o}C, 180 rpm) until reaching an OD_{595} of 0.7, at which point cell growth was arrested by chilling at 4 ^{o}C for 30 minutes. Cells were harvested by centrifuge (Heraeus Biofuge Prime R) at 3,500 *g* for 17 minutes at 4^{o}C. The cell pellet was washed twice by resuspension in 200 mL of ice cold dH_20 (Milli-Q) and pelleting at 6,000 *g* for 12 mins at 4 ^{o}C. This step was repeated twice with 100 mL of ice cold dH_20, and once with 20 mL of ice cold dH_20, before finally being resuspended in 6 mL of pre-chilled 30% (v/v) glycerol. Cells were then divided into 80 µL aliquots and snap frozen in liquid nitrogen for storage at -80 ^{o}C.

2.3.2 Transformation of Chemically Competent DH5*α* *E. coli*

An aliquot of calcium competent DH5*α* cells was thawed, mixed with 1 µL of plasmid DNA (50-100 ng/µL) and incubated on ice for 30 minutes. Cells were then heat shocked in a water bath at 42 ^{o}C for 30 seconds and returned to ice for a further 5 minutes. Cells were supplemented with 400 µL of SOC media (Fisher) and incubated at 37 ^{o}C for 1 hour (180 rpm), after which 150 µL of the culture was plated on ampicillin selective agar plates and grown overnight.

2.3.3 Transformation of Electrocompetent BL21 (DE3) *E. coli*

Electrocompetent BL21 (DE3) cells were thawed and gently mixed with 1 µL of plasmid DNA (50-100 ng/ µL). Following 2 minutes of incubation on ice the cells were transferred to a chilled 0.2 cm electroporation cuvette (Geneflow). A single 2.5 kV pulse was then applied to the cuvette by a MicroPulser Electroporator (Bio-Rad) and 1 mL of SOC added immediately. The culture was then placed into a sterile culture tube and incubated at 37 ^{o}C for 1 hour (180 rpm). A 200 µL sample of culture was subsequently plated on ampicillin selective agar plates and incubated overnight.

2.4. Gene Fragments

Synthetic gene fragments (See Supplementary Data) were ordered from Integrated DNA Technologies and supplied as dry gBlocks®. These gBlocks were resuspended to a working concentration of 10 ng/µL in nuclease free water (Thermo Scientific) as confirmed by NanoDrop Lite (Thermo Scientific) spectrophotometer at a wavelength of 260 nm.

2.5. Manipulations of DNA

2.5.1. Isolation of Plasmid DNA

DNA was extracted from 5 mL overnight cultures of DH5*α* *E. coli* with the Monarch Plasmid Miniprep Kit (New England Biolabs) as stated in the manufacturer's instructions. DNA concentration and purity were confirmed by NanoDrop Lite (Thermo Scientific) spectrophotometer (260nm, 260nm/280nm).

2.5.2. Restriction Digest of Plasmid

Endonuclease digestion of pET32a was performed with *Nco*I-HF (New England Biolabs) as per the manufacturer's instructions, except for an increased 1-hour incubation period. Following heat inactivation at 80 ^{o}C for 20 minutes, a sample was analysed by gel electrophoresis to confirm complete digestion. The linearized pET32a was then purified via PCR cleanup (New England Biolabs) and the concentration quantified by NanoDrop Lite.

2.5.3. Agarose Gel Electrophoresis

DNA electrophoresis was performed using a 1% w/v agarose (Promega) gel as described by Sambrook *et al.*[100], stained with 0.5 µg/mL of ethidium bromide and sizes estimated using a 1kb plus DNA Ladder (New England Biolabs). Gels were run in TAE Running Buffer (40 mM Tris, 20 mM Acetic Acid, 1 mM EDTA) at 100 volts for 30 minutes, then viewed by UV illumination with the Syngene G:box gel imager.

2.5.4. DNA Gel Extraction

DNA extraction from agarose gels was performed as specified by the Monarch DNA Gel Extraction Kit (New England Biolabs) and quantified by NanoDrop Lite.

2.5.5. PCR and DNA Cleanup

Monarch PCR and DNA Cleanup Kit (New England Biolabs) was used per manufacturer's instructions to purify *Nco*I digested pET32A and PCR amplification fragments. DNA was subsequently quantified by NanoDrop Lite.

2.6. Primers

Name	Sequence 5'→ 3'	Use
T7_FWD*	TAATACGACTCACTATAGGG	Sequencing and amplification from the T7 promoter
T7_REV*	GCTAGTTATTGCTCAGCGG	Sequencing and amplification from the T7 terminator
LSS_FWD*	TACCGACGACGACGACAAGGCGCTGCAACACATGAACATTC	Amplification of LSS Full or LSS M23 fragments and addition of 5' overlap region.
LSS_REV*	CGGATCCGATATCAGCCTTTATAGTTCCCCAAAGAAC	Amplification of LSS Full fragment and addition of 3' overlap region.
LSS_M23_REV*	ACCGGACCCCGATCCACCTATTTGATTACCTCCTC	Amplification of LSS M23 fragment and addition of 3' overlap region.
EGFP_FWD*	ACCGACGACGACGACAAGGCCATGGTGAGCAAGGGCGAG	Amplification of eGFP and addition of 5' overlap region.
EGFP_REV*	CCGCTACCGGACCCCGATCCACCGCCCTTGTACAGCTC	Amplification of eGFP and addition of 3' overlap region.
LSS_MB_FWD**	**C**GCTGCAACACATGAACATTCAG	SDM to restore reading frame of LSS-FULL and LSS-SH3b / LSS-Sort constructs.
LSS_MB_REV**	GCCTGGTCGTCGTCGTCG	SDM to restore reading frame of LSS-FULL and LSS-SH3b / LSS-Sort constructs.
LSS_STP_FWD*	**TAA**GCGATATCGGATCCGAATTC	SDM to add stop codon to 3' end of reading frame of LSS-FULL construct.
LSS_STP_REV*	CTTTATAGTTCCCCAAAGAAC	SDM to add stop codon to 3' end of reading frame of LSS-FULL construct.

Table 1. Primers used throughout the project. Overhang sequences added for HiFi assembly are shown underlined and insertion bases in bold. *Primers were supplied desalted or HPLC purified by Sigma and resuspended in nuclease free water to a stock concentration of 100 µM. **Primers were supplied desalted by Integrated DNA Technologies in IDTE (10 mM Tris, 0.1 mM EDTA, pH 8.0) at 100 µM. SDM = Site-Directed Mutagenesis

2.7. Molecular Cloning

2.7.1. PCR

Polymerase chain reactions were performed in a Thermo Scientific Hybaid HBSP02110 thermocycler, using Hot Start Q5 High-Fidelity DNA Polymerase (New England Biolabs) for cloning and site-directed mutagenesis (SDM); and One*Taq* Quick Load 2x Master Mix with Standard Buffer (New England Biolabs) for Colony PCR. Reactions were performed as detailed by the manufacturer's instructions in 25 µL reaction volumes for 30 cycles. Primer stocks were diluted in nuclease free water to 10 µM and annealing temperatures were predicted by TM calculator (New England Biolabs). Amplified DNA fragments were analysed by gel electrophoresis and fragments for cloning purified for downstream use by either PCR clean up or gel extraction based on homogeneity.

2.7.2. HiFi Assembly

DNA fragments were assembled into constructs within the pET32a vector using protocols specified by the NEBuilder HiFi DNA Assembly Master Mix (New England Biolabs). Vector:Insert ratios of 1:2 were used with approximately 20 fmoles of pET32a mixed with approximately 40 fmoles of gene fragments, except for the Sh3B gBlock which at <200bp's was used at a 1:5 ratio of approximately 100 fmoles. Resulting reactions were all within the recommended 0.03-0.2 pmoles of total fragments. Reactions were incubated at 50 ^{o}C for 1 hour and 2 µL of the product transformed into DH5*α* chemically competent cells.

2.7.3. Q5 Site-Directed Mutagenesis

Simultaneous kinase, ligase, and *Dpn*I treatment was performed on 1 µL of Q5 PCR products at 37 ^{o}C for 1 hour as detailed by the Q5® Site-Directed Mutagenesis Kit (New England Biolabs). The resulting product was then transformed into DH5*α* electrocompetent cells supplied with the kit.

2.8. Screening of Recombinant Clones

2.8.1. Colony PCR

Colonies of HiFi transformants were picked from agar plates and used to prime PCR reactions. PCR was performed with T7_FWD (5'-TAATACGACTCACTATAGGG-3') and T7_REV (5'-GCTAGTTATTGCTCAGCGG-3') primers using an annealing temperature of 45 ^{o}C and an extension time of 2 minutes, with the resulting products analysed by electrophoresis.

2.8.2. DNA Sequencing

To confirm successful cloning, 5µL (100 ng/µL) of plasmid DNA was sent to Source BioScience (Nottingham) for sequencing using T7_FWD and T7_REV primers supplied by Source BioScience. Sequencing results were provided in AB1 file format and chromatograms viewed in SnapGene Viewer. Trimmed sequences were then exported to Benchling for alignment and sequence verification.

2.9. Expression, Purification and Analysis of Recombinant Proteins

2.9.1. Small Scale Test Expressions

A colony of transformed BL21(DE3) was selected and used to inoculate 5 mL of sterile LB supplemented with 100 µg/mL ampicillin and grown overnight. 1mL of this culture was then used to inoculate 50 mL of LB (ampicillin) and a glycerol stock prepared. The 50 mL culture was incubated at 37 ^{o}C with shaking (180 rpm) until reaching an optical density (595nm) of 0.3, where upon a 1 mL uninduced sample was taken and the remaining divided into two 25 mL cultures. Each culture was then induced with IPTG to a final concentration of 1 mM and further incubated for 4 hours at 15 ^{o}C, 20 ^{o}C, or 30 ^{o}C. After incubation optical density of the cultures were recorded again and a sample consisting of a proportional number of cells (1000 µL/OD_{595}) was taken for analysis. Uninduced and induced samples were centrifuged (Heraeus Biofuge Pico) at 13,000 rpm, the supernatant removed, and the cell pellet frozen at -20 ^{o}C overnight.

Following sample pellet thawing, cell pellets were resuspended in 200 µL CelLytic B (Sigma), 1 µL of 50 mg/mL Lysozyme (Sigma), 0.5 µL Benzonase (250 ≥ units/µL) (Sigma), 3 µL 1M $MgCl_2$. Induced samples were then centrifuged (13,000 rpm, Heraeus Biofuge Pico) and the supernatant extracted to form the soluble fraction. The remaining pellet was resuspended in 20 mM Tris (pH 8.0) to create the insoluble fraction. All samples were then combined with 6x SDS loading buffer (400 mM Dithiothreitol (DTT), 200 mM Tris. 8% (w/v) SDS, 40% (w/v) glycerol and 0.4% (w/v) bromophenol blue) and denatured at 95 ^{o}C for 5 minutes. Samples were then analysed by SDS PAGE (Sodium Dodecyl Sulphate Polyacrylamide Gel Electrophoresis).

2.9.2. Large Scale Over Expression

A 10 mL culture was inoculated from the glycerol stock produced during test expressions and shaken (180 rpm) overnight at 37 ^{o}C. This culture was then used to inoculate 1 L of LB (100 µg/mL ampicillin), which was grown to an optical density (595nm) of 0.6-0.8. An uninduced sample (1 mL) was taken before induction with IPTG (1 mM) and the culture incubated overnight at the selected temperature.

Cells were harvested by centrifugation using a Beckman Avanti J-25 I with a JLA 10.500 rotor at 4500 *g* for 12 mins at 4 ^{o}C. Cell pellets were resuspended in Buffer A (20 mM Tris, 15 mM Imidazole, 300 mM NaCl) and lysed using a Soniprep 150 sonicator (Sanyo). Sonication was performed on ice with the 19mm probe. Applying 30-second pulses of 15 µm Amps of sonication interspaced by 30 second cooling periods for a total of 10 minutes. Lysate was then immediately centrifuged using an Avanti J-26S XP (Beckman) with a JA-25.50 rotor at 35,000 *g* for 35 minutes. The soluble fraction was removed for purification and the insoluble fraction resuspended in 8M urea and a sample mixed with 6x SDS loading buffer for SDS PAGE analysis.

2.9.3. Purification of Recombinant Protein

Protein purification was performed using a 5 mL HisTrap HP (GE Healthcare) Ni IMAC column with an AKTA Start (GE Healthcare) FPLC platform using UNICORN (GE Healthcare) control software. The HisTrap HP column was equilibrated with 20 mL of Buffer A (20 mM Tris, 15 mM Imidazole, 300 mM NaCl) before loading the lysate at 2 mL/min, collecting the flow through for analysis. Additional buffer A was washed through the column to remove weakly bound protein until UV (280nm) absorbance returned to baseline levels. Protein elution was then performed by a stepped or gradient increase in Buffer B (20 mM Tris, 700 mM Imidazole, 300 mM NaCl) concentration from 0-100%, with the elution collected in 10 mL fractions. Fractions with high UV absorbance were then analysed by SDS PAGE for the presence of the protein of interest.

2.9.4. SDS PAGE

SDS PAGE analysis of denatured protein samples was performed using the BioRad mini-PROTEAN gel casting system and electrophoresis cell. 12% acrylamide gels (12% Resolving, pH 8.8; 5% Stacking, pH 6.8) were prepared and submerged in SDS Running buffer (25 mM Tris-HCl, 200 mM glycine, 0.1% (w/v) SDS). Protein samples denatured in SDS loading dye were then loaded onto the gel along with PageRuler Plus pre-stained protein ladder (Thermo Scientific). 180 volts were applied for 10 minutes to condense the samples at the stacking-resolving boundary, whilst a further 200 volts for 50 minutes to separate proteins by molecular weight. Excess SDS was removed by submerging the gel in RO (reverse osmosis) water and microwaving at low power (defrost setting) for 2 minutes.

The washed gel was then submerged in GelCode Blue Safe Protein Stain (Thermo Scientific), microwaved on defrost setting for 5 minutes and allowed to stand for a further 5. Excess stain was removed from the gel by three rounds of washing in RO water and microwaving for 2 minutes before being agitated in RO water overnight. The de-stained gel was then visualized under white light using the G:box gel imager (Syngene).

2.9.5. Protein Storage

Fractions containing protein of interest were combined and dialyzed into 20 mM Tris (pH 8) overnight using Spectra/Por 6-8 kD MWCO dialysis tubing (Fisher Scientific). Dialyzed proteins were concentrated by spin concentration or PEG dialysis before sample aliquoting and storage at -80 ^{o}C. Spin concentration of eGFP-Sort was performed using Vivaspin 20ml (10,000 MWCO) spin concentrators (GE Healthcare). Whilst PEG dialysis of eGFP-SH3b was performed using 30% 20,000 Polyethylene Glycol (Sigma).

2.9.6. Determination of Protein Concentration

Protein concentration was calculated using the Beer-Lambert Law:

$$\mathbf{C = A / \varepsilon b}$$

Where C is concentration (M), A is absorbance (A), ε is the molar absorptivity coefficient ($M^{-1}cm^{-1}$), and b is path length in centimetres (cm).

Absorbance was measured at 280 nm with a NanoDrop Lite which has a path length of 1 cm, and the molar absorptivity coefficient predicted by the ProtParam tool[101].

3. Results and Discussion

3.1. Linearization of pET32a

The plasmid pET32a was chosen as a universal vector for both the cloning and expression of LSS and a library of fusions proteins. Using the HiFi assembly cloning method, expression constructs were generated by the inserting gene fragments into pET32a. These fragments were inserted at the *Nco*I restriction site, situated within the larger multiple cloning region. Expression of the inserted construct would be under the regulation of a lac inducible promoter and be translated downstream of a cleavable N-terminal region containing both solubility and his-purification tags (see Figure 4b). Unlike a standard restriction digest based cloning strategy, HiFi assembly does not utilise endonucleases. Instead using an exonuclease, HiFi requires the plasmid to be linearized prior to the assembly reaction.

Plasmid pET32a was successfully linearized by a single *Nco*I restriction digest as shown by Figure 5. It was important that the digest was as complete as possible because any circular entering the HiFi reaction would remain in the products being transformed into competent cells. Without a phenotypic screening method available to readily distinguish clones possessing the insert from those without, it would be required that clones be screened by PCR. To avoid this, attempts were made to alternatively linearize the backbone by PCR amplification with subsequent *Dpn*I treatment to remove the circular template plasmid. However, due to difficulties in designing appropriate primers and the need to further screen transformants anyhow, a restriction digest was sufficient.

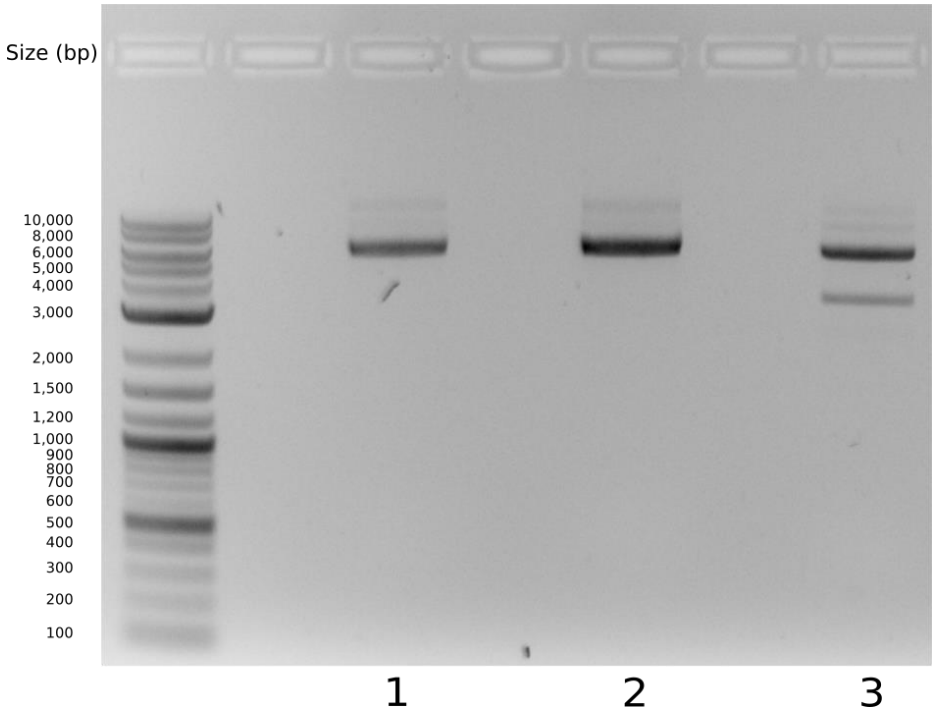


Figure 5. Electrophoresis of pET32a *Nco*I digestion products. Lanes 1 and 2 show restriction products whilst lane 3 shows an uncut pET32a control. Because supercoiled DNA migrates faster than linear DNA, the dark band in lane 3 appears fractionally lower than those in lanes 1 and 2. Faint bands observed in all three lanes represent nicked and dimerized DNA, whilst the lower band in lane 3 likely represents circular ssDNA produced during the alkaline lysis of DH5α cells.

3.2. Amplification of eGFP

Amplification of eGFP was performed to produce fragments for the assembly of eGFP - SH3b / Cws fusion expressing constructs. These fusions are designed for future cell-wall binding assays to compare the affinity of each cell wall binding domain, and to assess whether the outer cell wall of *S. aureus* is permeable to a protein of the approximate size of a catalytic domain. eGFP was successfully amplified by PCR and purified by PCR clean up. Electrophoresis of the amplification products showed the presence of a single product of the approximate 722 bp size expected for eGFP (see Figure 6). Although PCR products could have been used directly in HiFi assembly, the decision was made to clean up the fragment to remove any contaminating polymerase, nucleotides, and primers. Where PCR was performed in two 25 µL reaction volumes the products of both were combined.

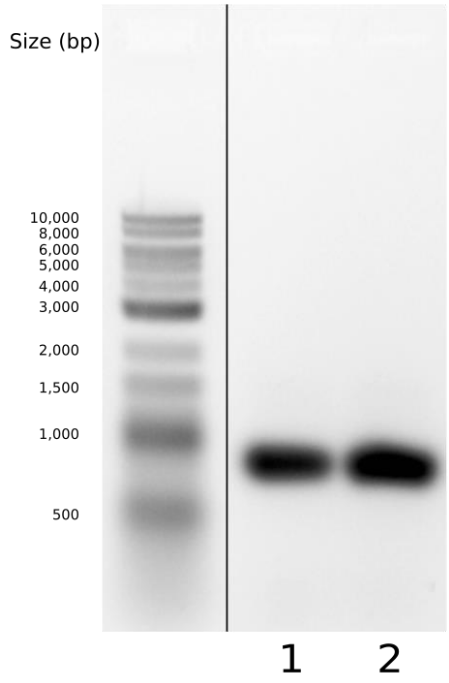


Figure 6. Amplification of eGFP. Two 25 µL PCR's were performed using primers EGFP_FWD (5'ACCGACGA CGACGACAAGGCCATGGTGAGCAAGGGCGAG-3') and EGFP_REV (5'-CCGCTACCGGACCCCGATCCACCGCCCTT GTACAGCTC-3') with an annealing temperature of 72 ^{o}C and extension time of 30 seconds. Fragments approximately match the expected eGFP fragment size of 722 bp. #The black line demarks the cropping of intervening lanes containing pET32a digest samples (not shown).

3.3. Amplification of LSS Fragments

LSS-Full encoding the full sequence of the mature LSS protein was amplified so to provide both a positive control and a benchmark for assaying the catalytic activity of the domain fusions in future turbidity assays. Additionally, the M23 catalytic domain was amplified so SH3b and Cws fusions could be assembled and expressed to elucidate the impact of altering the linker and the cell wall binding domain.

3.3.1 Amplification of LSS Full

The full length LSS sequence encoding the native LSS protein was amplified from pET30a-LSS (See Figure 7). Amplification was performed with LSS_FWD (5'-TACCGACGACGACGACAA GGCGCTGCAACACATGAACATTC-3') and LSS_REV (5'-CGGATCCGATATCAGCCTTTAT AGTTCCCCAAAGAAC-3') primers. An annealing temperature of 68 ^{o}C and an extension time of 30 seconds were found to be optimal for the 775 bp fragment. Again, PCR products from two 25 µL reactions were combined and cleaned up to increase the yield.

3.3.2 Amplification of LSS M23

Two steps were required to obtain a homogenous LSS M23 domain amplification product, because the initial amplification reaction shown in Figure 7 resulted in the production of a second fragment of approximately 800 bp. Upon examining the pET30a-LSS template sequence it can be observed that the region immediately downstream of LSS has a region that shares homology with the 3' overhang sequence found in the LSS_M23_REV (5'-ACCGGACCCCGATCCACCTATTTGATTACCTCCTC-3') primer. The hypothetical product from LSS_M23_REV mis-annealing to this site whilst LSS_FW (5'-TACCGACGACGACGACAAGGCGCTGCAACACATGAACATTC-3') correctly anneals would be 777 bp in size, suggesting this is in fact what occurred. To resolve this, gel extraction was used to extract the desired 240 bp band and a second round of PCR performed to increase the yield. The second round produced a single band of the expected 240 bp size making it suitable for PCR clean up and assembly (see Figure 8). In both PCR reactions the annealing temperature was optimized to 65 ^{o}C and a 30 second extension cycle used.

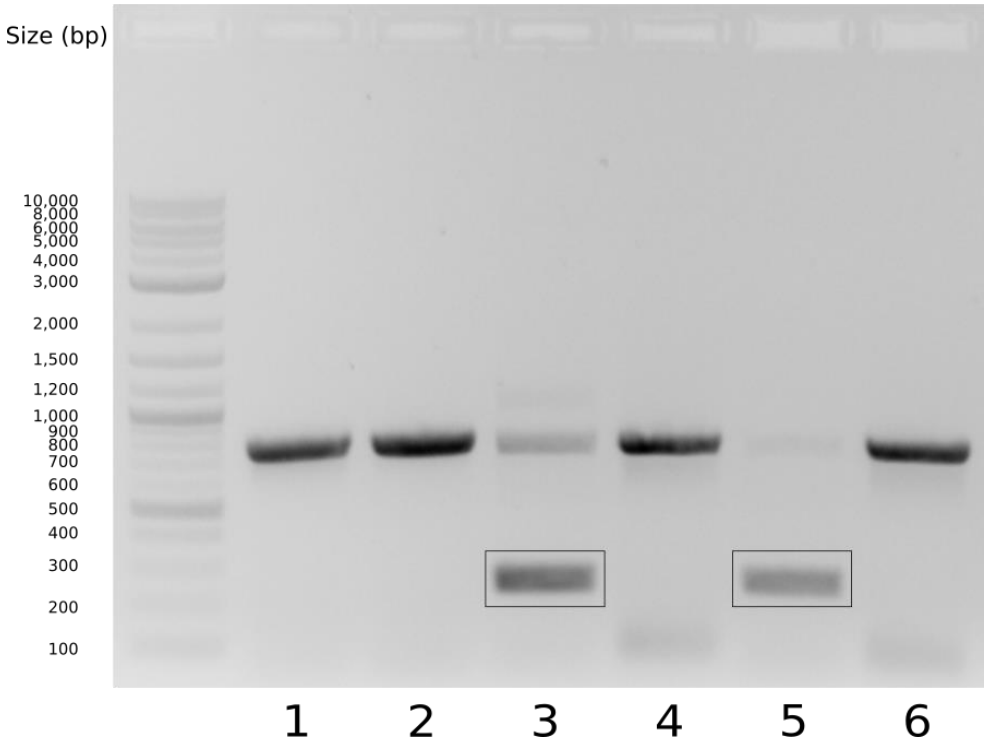


Figure 7. The production of homogenous full length LSS and heterogeneous LSS M23 gene fragments amplified from pET30a-LSS (6695 bp). Lanes 1 and 2 show the LSS-Full amplification product (775 bp). Lanes 3 and 5 show the two (primary) amplification products from the initial LSS M23 fragment amplification (240bp). The bands outlined were excised and extracted from a fresh gel (not shown) to reduce UV exposure. Lanes 4 + 6 show the amplification of eGFP that was unused due to redesigning of the primers.

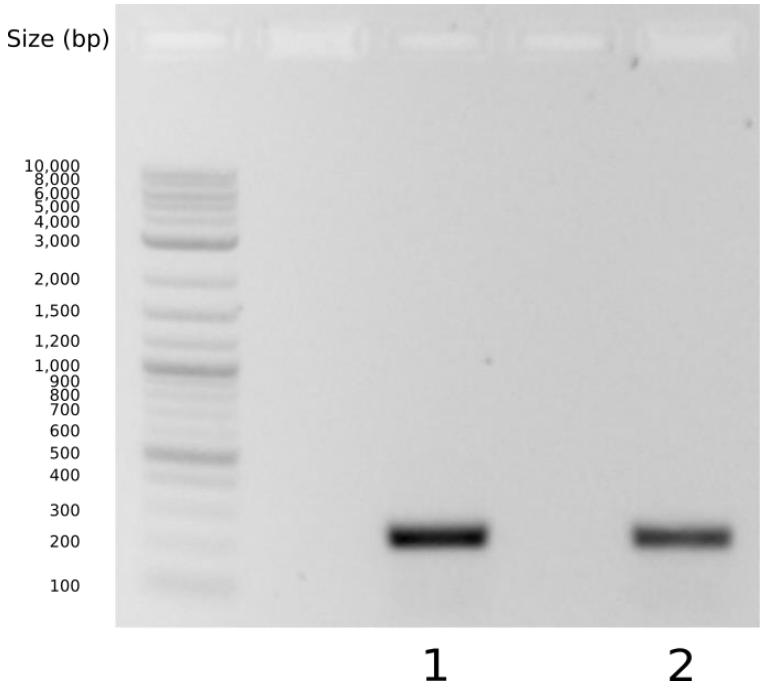


Figure 8. Amplification of the LSS M23 domain fragment. Lanes 1 and 2 represent two 25 µL PCR reactions set up with the 240 bp fragment excised from the first reaction. The resulting individual band confirms undesired annealing was due to a region in the original template.

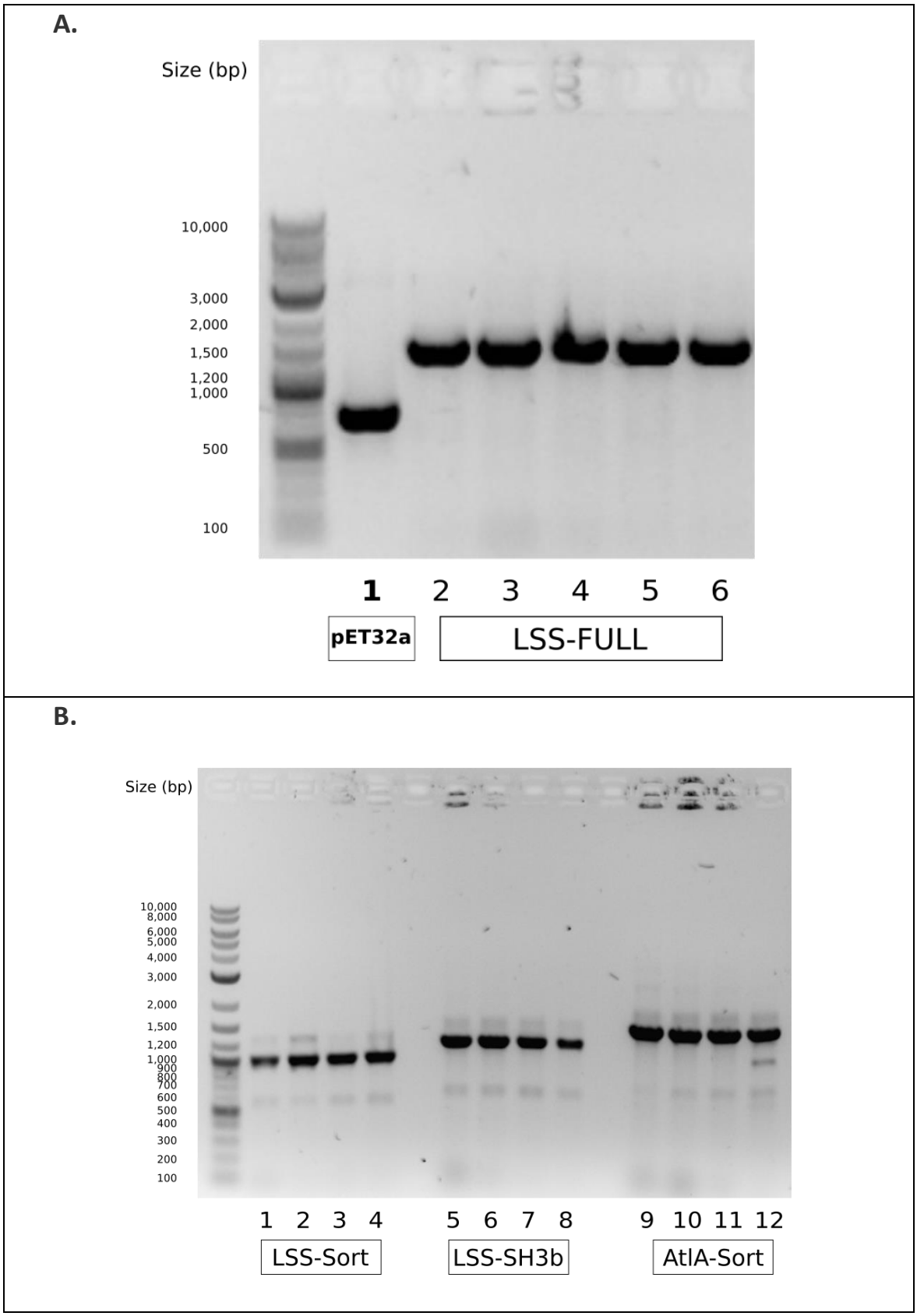
3.4. HiFi Assembly of Gene Constructs

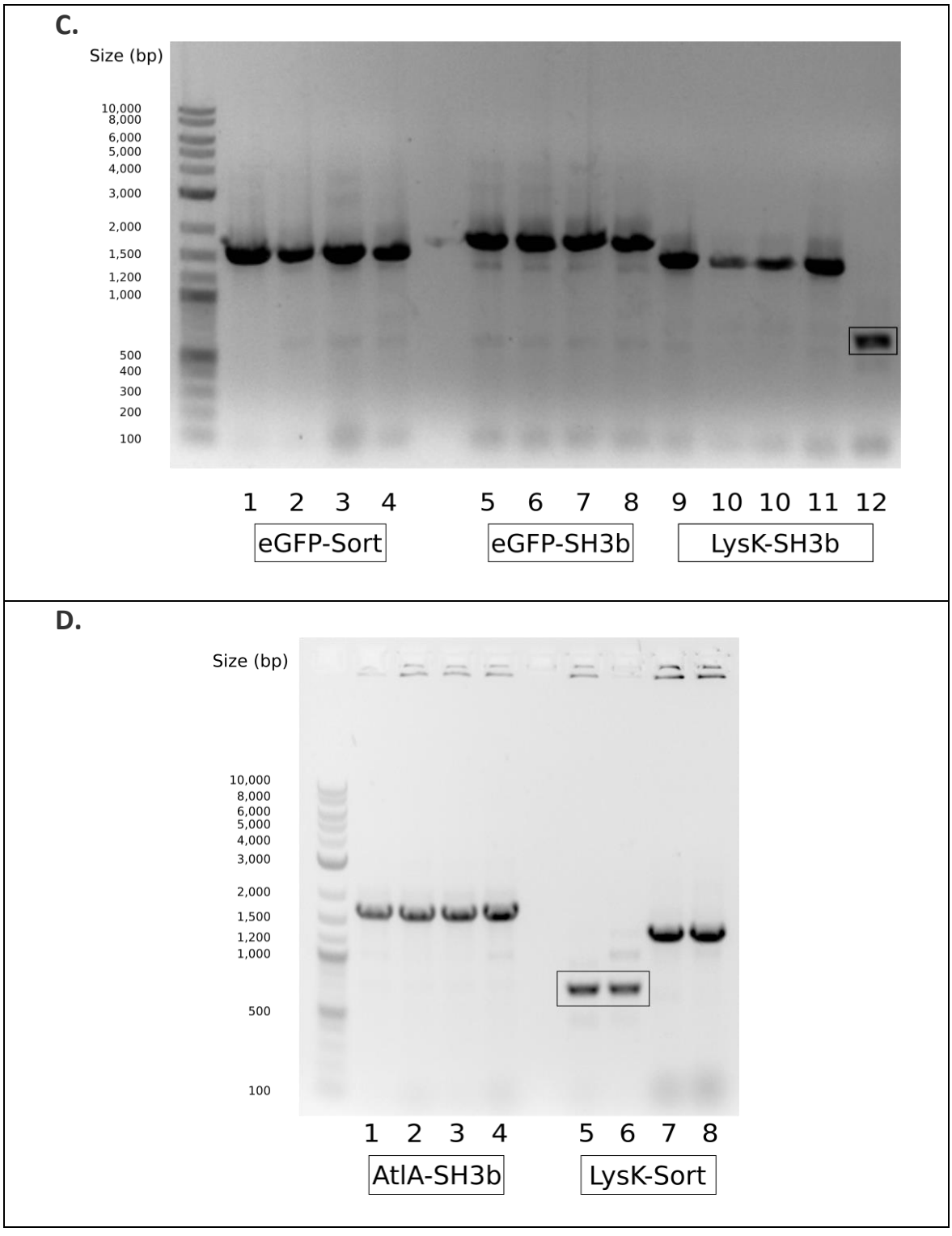
Adding the amplified LSS-Full, LSS-M23 and eGFP fragments to the collection of synthesised catalytic, SH3b and Cws domains, a library of DNA constructs was assembled. The individual catalytic domain fragments / eGFP were assembled both with either the SH3B or Sort-tag fragments, whilst LSS-Full was assembled alone into pET32a. The initial step of the HiFi assembly reaction involves the generation of 3' overhangs by a 5'-3' exonuclease. These 3' overhangs at the ends of the linear plasmid and insert fragments anneal due to regions of homology introduced to the inserts during fragment amplification / synthesis. A polymerase uses the annealed sequence as a template to extend the 3' ends resulting in the two pieces of DNA being joined by two single-strand nicks. The last step of HiFi is ligation of the nicks by a nick-specific ligase resulting in a single double-stranded piece of DNA. With this happening at either end of the plasmid and each fragment, successful assembly results in a circularised plasmid containing a directionally orientated insert.

To verify the successful assembly of these constructs, reaction products were first transformed into competent cells and screened by performing colony PCR with T7_FWD (5'-TAATACGACTCA CTATAGGG-3') and T7 REV (5'-GCTAGTTATTGCTCAGCGG-3') primers. This allowed for amplification across the insert site, which when examined by gel electrophoresis, revealed whether an insertion event had taken place and the size of the inserted sequence. From this, it was determined whether each clone represented a potential successful assembly. During this screening, several colonies did produce amplification products of approximate size of the 712 bp region found within the original pET32a backbone (See Figures 9c and 9d). The removal of the 5' sticky-ends; produced during the *Nco*I restriction digest, by the 5'-3' exonuclease along with the high specificity of the HiFi ligase should have prevented pET32a re-linearizing. Suggesting that the linearization of pET32a had not been complete. Resulting in a small population being transformed with the empty pET32a. Despite this, screening did identify candidates for the successful assembly of LSS-Full (see Figure 9a); LSS-Sort, LSS-SH3b, AtlA-Sort (see Figure 9b); eGFP-Sort, eGFP-SH3b, LysK-SH3b (see Figure 9c); AtlA-SH3b, LysK-Sort (see Figure 9d) ;HydH5-Sort, and HydH5-SH3b (see Figure 9e).

Although the PCR results suggested that the insertion of gene fragments was successful, it was necessary to confirm the orientation and sequence of the assembly. Because of the read length of sanger sequencing is limited to approximately 1 kb, constructs with sequences > 1 kb from the T7 terminator to the 5' overlap region were sequenced from both the T7 promoter and terminator to get full coverage of the insert. Where this distance was < 1kb constructs were sequenced from the terminator only.

Sequencing showed that the fragments did indeed insert within the right orientation as expected, and assembly had generated at least one successful transformant for each construct. However, several candidates did display small base insertion or deletions (INDELs) within the overlap regions. These INDELs likely originated during gBlock synthesis. This is because both the proprietary and Q5 polymerase; used in HiFi assembly and gene amplification respectively, are hi-fidelity proof-reading polymerases. Small INDELs identified downstream of the stop codon within the distal overlap region were considered neutral and the assembly treated as successful. This is because they did not affect the coding sequence nor disrupt any known 3' UTR region features.


A.
Size (bp)
10,000
3,000
2,000
1,500
1,200
1,000
500
100
1 2 3 4 5 6
pET32a
LSS-FULL
B.
Size (bp)
10,000
8,000
6,000
5,000
4,000
3,000
2,000
1,500
1,200
1,000
900
800
700
600
500
400
300
200
100
1 2 3 4 5 6 7 8 9 10 11 12
LSS-Sort
LSS-SH3b
AtlA-Sort


C.
Size (bp)
10,000
8,000
6,000
5,000
4,000
3,000
2,000
1,500
1,200
1,000
500
400
300
200
100
1 2 3 4 5 6 7 8 9 10 10 11 12
eGFP-Sort
eGFP-SH3b
LysK-SH3b
D.
Size (bp)
10,000
8,000
6,000
5,000
4,000
3,000
2,000
1,500
1,200
1,000
500
100
1 2 3 4 5 6 7 8
AtlA-SH3b
LysK-Sort

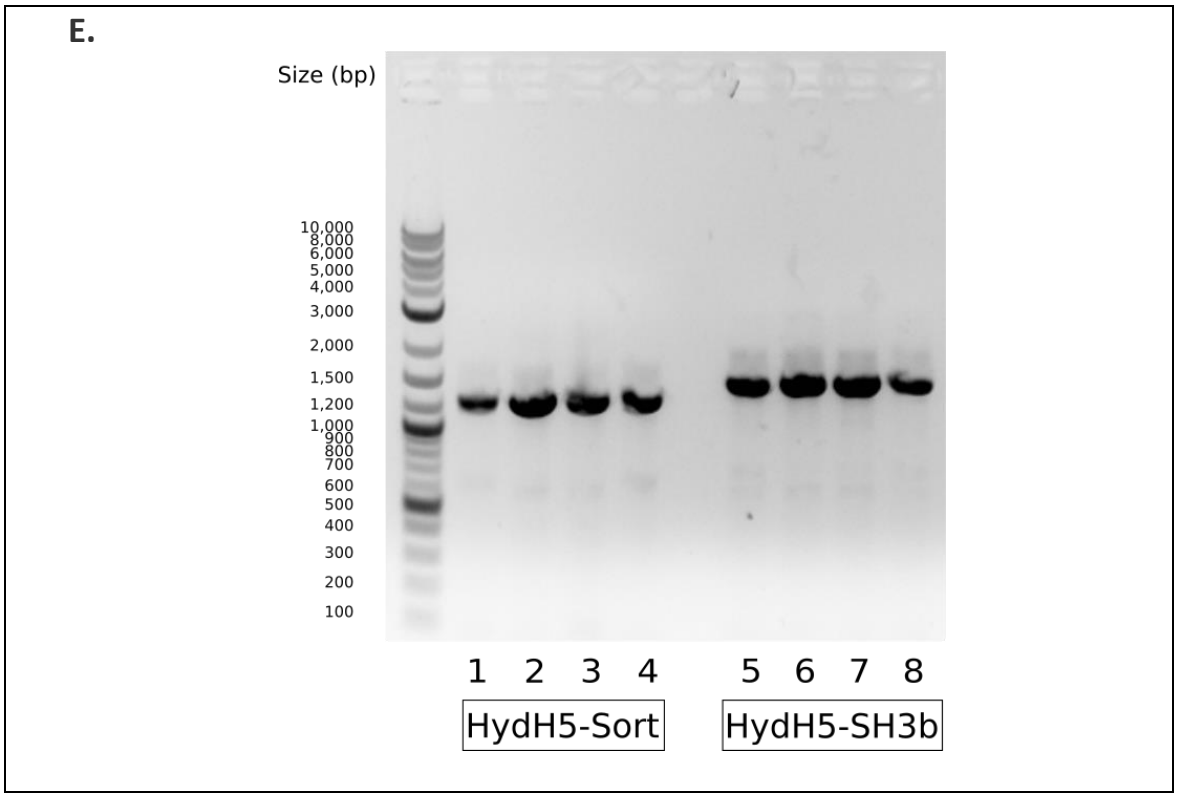


Figure 9. Colony PCR screening of HiFi transformants. A) Lane 1: pET32a vector (712 bp), Lanes 2-6: LSS-Full (1,445 bp). B) Lanes 1-4: LSS-Sort (1,031 bp), Lanes 5-8: LSS-SH3b (1,233 bp), Lanes 9-12: AtlA-Sort (1,502 bp). C) Lanes 1-4: eGFP-Sort (1,550 bp), Lanes 5-8: eGFP-SH3b (1,752 bp), Lanes 9-12: LysK-SH3b (1,515 bp). D) Lanes 1-4: AtlA-SH3b (1,704 bp), Lanes 5-8: LysK-Sort (1,313 bp). E) Lanes 1-4: HydH5-Sort (1,268 bp), HydH5-SH3b (1,470 bp). Incorrect band sizes representing re-circularization of pET32a are boxed.

3.5. Mutagenesis of LSS Constructs

When confirming the sequence of positively screened clones, sequencing identified two issues with the resulting LSS constructs (FULL, SH3b and Sort). Firstly, a single base deletion within the upstream overlap region, adjacent to the inserted LSS fragment was observed in candidates from all three constructs. This deletion of a single cytosine would have produced a deleterious frame shift, so mutagenesis was performed to reinsert this base. Secondly, when sequencing LSS Full constructs James Kapp (PhD student in the Thomas group) identified that all candidates were missing a stop codon. Again, mutagenesis was performed by James Kapp to introduce a stop codon to the end of the LSS Full coding sequence.

3.5.1 Restoration of Reading Frames

SDM restored the reading frames of LSS-Full, LSS-SH3b and LSS-Sort as confirmed by sequencing. To confirm that amplification of the HiFi templates was occurring, amplification products were run on electrophoresis gels. This allowed for the optimization of LSS_MB_FWD (5'-CGCTGCAA CACATGAACATTCAG-3') and LSS_MB_REV (5'-GCCTGGTCGTCG TCGTCG-3') primer annealing temperatures as can be seen in Figure 10b. However, the resolution of the agarose gel is too small to see a difference between the original template and the mutated sequence. This can be seen in Figure 10a, where amplification products migrate the same as LSS-Full template. Therefore, sequencing was required to confirm the presence of the desired mutation.

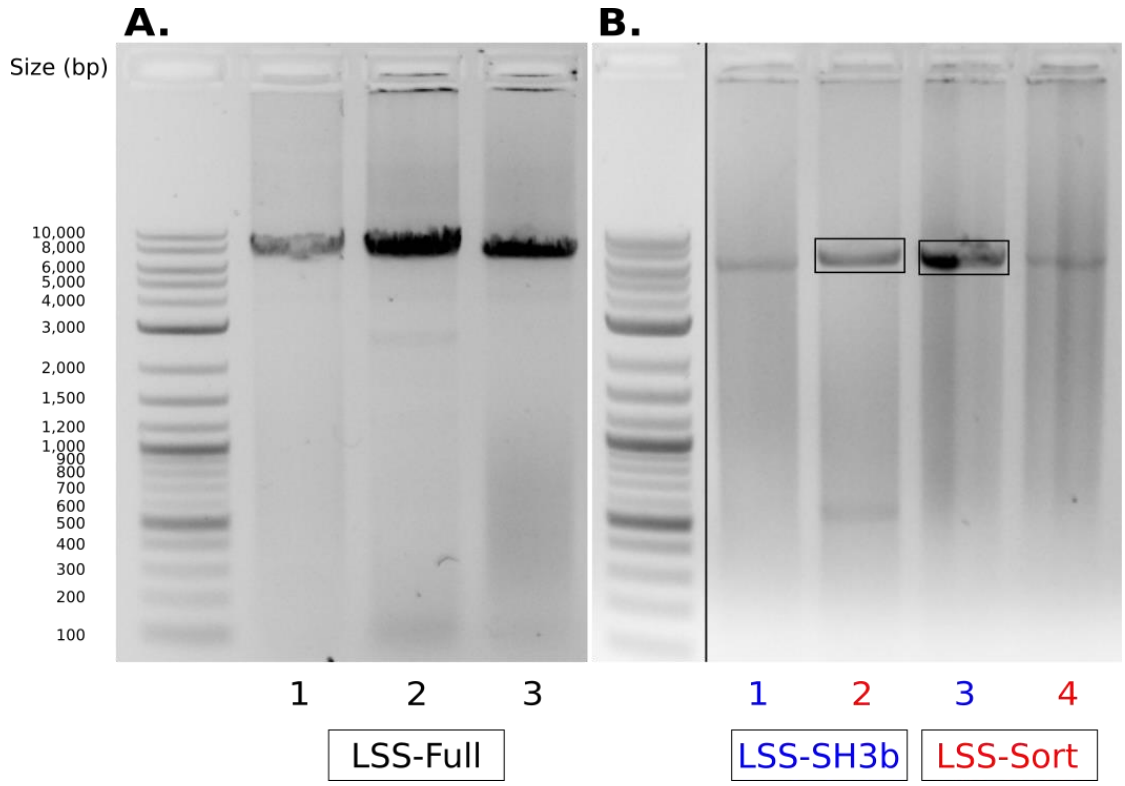


Figure 10. Site-Directed Mutagenesis products. A) Lane 1: LSS-Full control, Lanes 2-3: Mutated LSS-Full. Annealing temperature 65 ^{o}C, Extension Time 3.5 minutes. B) Lanes 1 + 2: Mutated LSS-SH3b, Lanes 2 + 4: Mutated LSS-Sort. 63 ^{o}C (1+2) and 67 ^{o}C (3+4) annealing temperatures were tested with 63 ^{o}C being optimal for LSS-SH3b and 67 ^{o}C for LSS-Sort.

3.5.2 Insertion of Stop Codon

Unlike the other pET32a constructs, assembly of the LSS-Full construct did not include either of the SH3b and Sort-tag gBlock fragments. These fragments had been designed to include a terminal stop-codon that would terminate translation immediately after the SH3b or sort-tag. However, the primers used to amplify the full length LSS fragment did not contain such a stop codon. Therefore, translation of the initial LSS-Full assembly construct would have resulted in translation terminating downstream of the end of the LSS sequence, producing an additional C-terminal his-tag (see Figure 4b). Among other unexpected effects, the presence of this uncleavable C-terminal his-tag could potentially disrupt the binding affinity of the SH3b domain. As such, SDM was performed by James Kapp using the LSS_STP_FWD (5'-TAAGCGATATCGGATCCGAATTC-3') and LSS_STP_REV (5'-CTTTATAGTTCCCCAA AGAAC-3') primers to introduce a TAA stop codon immediately downstream of the full LSS sequence (see Figure 11).

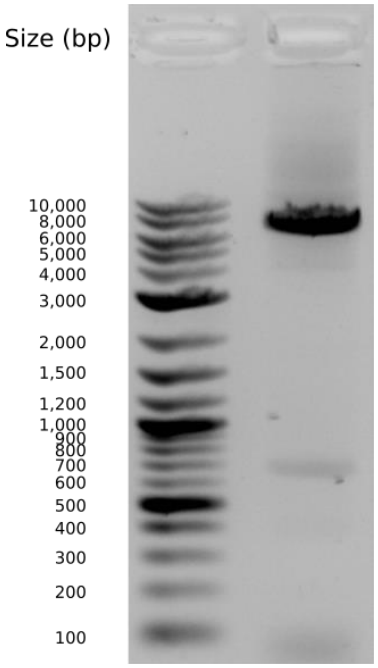


Figure 11. LSS-Full site directed mutagenesis products demonstrate successful amplification of construct. Mutagenesis was optimized to an annealing temperature of 65 °C and an extension time of 3.5 minutes. The faint band around 700 bp likely represents a secondary product produced by non-specific primer binding. This secondary product if annealed was too small to contain both the AmpR and origin of replication so would not be maintained within a cell. It would therefore have been screened out during transformation.

3.6. Expression of eGFP constructs

The eGFP- Sort and eGFP- SH3b fusions were expressed and purified for use in future cell wall binding studies to qualify and quantify the integration of exogenous sort-tagged protein into the Staphylococcal cell wall by endogenous SrtA, as well as to compare this to the binding dynamics of the SH3b domain. Once expression conditions were identified in small scale test expression tests the fusion proteins were overexpressed to provide quantities of protein that could be purified and used in cell wall binding assays.

3.6.1 Test Expression of eGFP-Sort

Expression tests were performed on eGFP-Sort to establish the conditions for overexpression. Initially, 30 ^{o}C was investigated for expression but the protein displayed a high degree of insolubility (see Figure 12a). Lowering the incubation temperature to 15 ^{o}C or 20 ^{o}C reduced the proportion of insoluble protein, with little observable difference in protein output (see Figure 12b). A dark band can also be seen between 10 and 15 kDa in the insoluble lane of Figure 12a. Although unclear due to gel warping, this band may also be present within the soluble fraction and would likely reflect a truncation event.

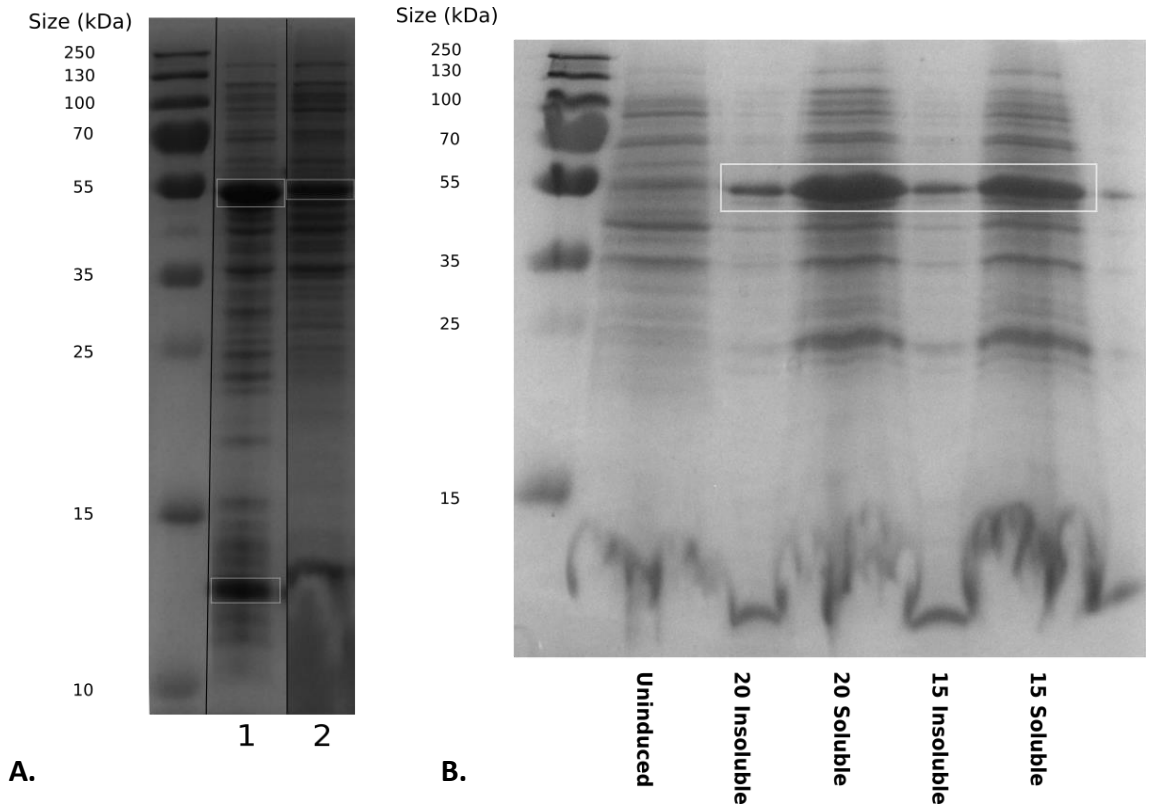


Figure 12: Test expression of eGFP-Sort. A) Insoluble (Lane 1) and Soluble (Lane 2) fractions of BL21 (DE3) cells expressing eGFP-Sort at 30^{o}C for 4 hours. B) Whole cell lysate of uninduced cells, soluble and insoluble fractions from expression cultures incubated at either 20 or 15 ^{o}C. eGFP-Sort and truncation are shown in boxes. Mw of eGFP-Sort = 47.9 kDa.

3.6.2 Overexpression of eGFP-Sort

Overexpression was performed at 15 ^{o}C and purification of eGFP-Sort was performed by two rounds of Ni-IMAC. The chromatogram in Figure 13 shows that following the first step in (10%) Buffer B concentration the UV absorbance sharply peaked. Fractions 2 and 3 when examined on the SDS PAGE gel show little protein other than the desired 47.9 kDa eGFP-Sort. However, in fractions 4 the presence of other proteins increased along with that of eGFP-Sort. This could have been caused by the concentration of Buffer B in the system taking time to equilibrate, causing the very weakly bound eGFP-Sort to be washed off below 10% Buffer B. This washing off of eGFP-Sort at such low imidazole concentrations suggests that the column matrix was saturated, providing only weak interactions with these proteins. Fractions 7 through to 19 whilst demonstrating high eGFP concentrations appear to contain higher concentrations of unwanted proteins. Interestingly these included two prominent bands approximately 25 kDa in size. This could represent possible His-Tagged truncations. Analysing the codon usage of the eGFP-Sort supports this, showing the presence of three rare proline encoding CCC codons. With the predicted truncation products resulting from premature termination at these CCC codons having a molecular weight of approximately 23 kDa. Another prominent band can be found between 100 and 120 kDa. This likely represents eGFP dimerization, a property known to occur at high concentrations. Whilst it is apparent that most of the protein was eluted during the 10 - 60% gradient wash, fraction 29 shows that a small amount of eGFP-Sort was still bound prior to the final 100% wash step.

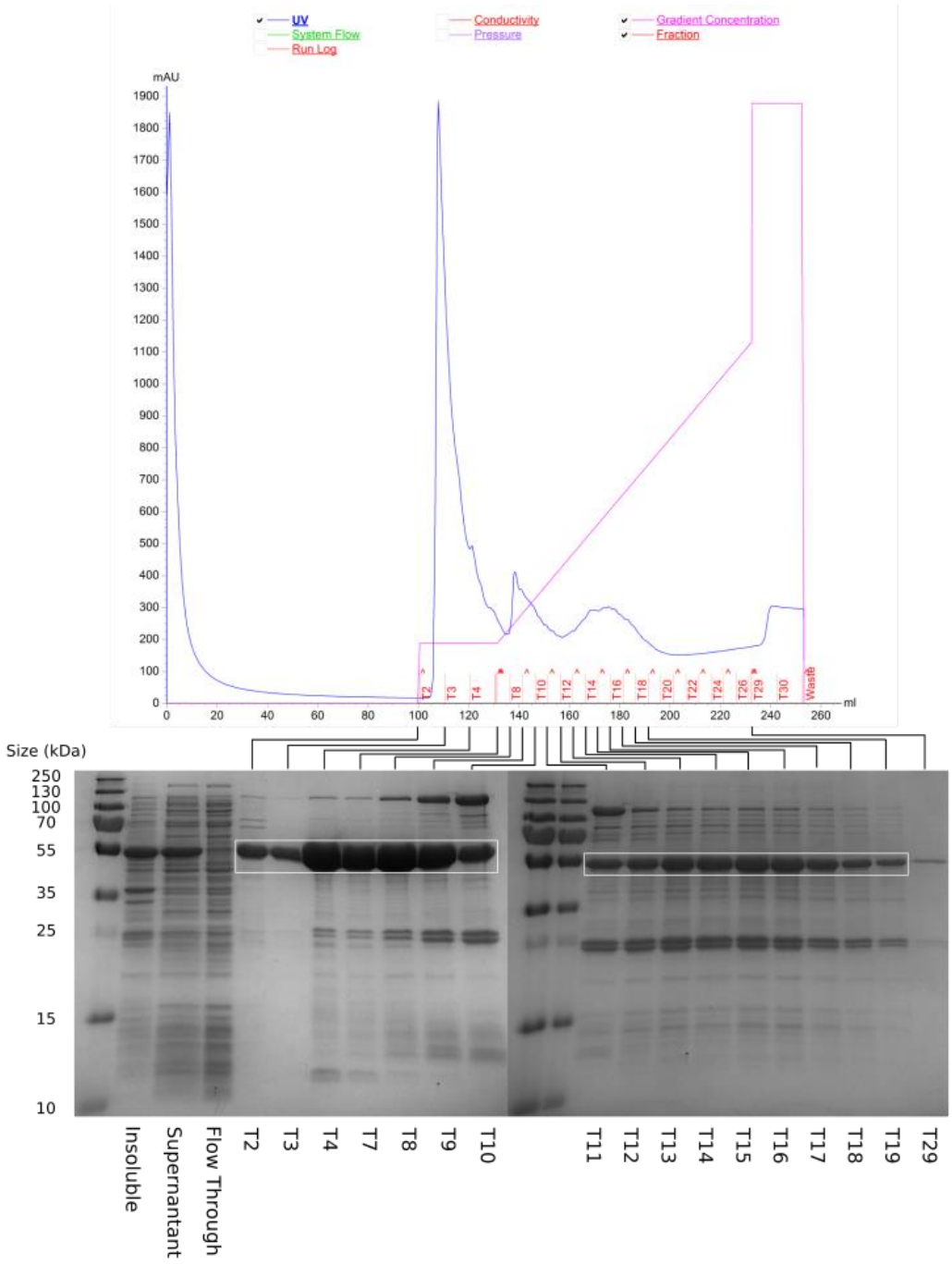


Figure 13. Initial IMAC purification of eGFP-Sort. The chromatogram displays the UV absorbance of column flow through being collected in 10 mL fractions (red) through the increasing Buffer B concentration gradient (Pink). The SDS PAGE gels show the proteins presence in these fractions, proteins that did not bind during loading (Flow Through), and both insoluble and supernatant fractions following lysis. Fractions showing high concentrations of eGFP-Sort (Mw 47.9 kDa) are highlighted.

Because of the high degree of contamination in the fractions obtained during the initial purification a second purification step was performed. Fractions 2 through to 19 were combined and re-dialysed into Buffer A to be re-purified. Figure 14 shows that this combined sample primarily consisted of eGFP-Sort along with the hypothetical truncations. During the second purification a step gradient approach was used to try to obtain just the full eGFP-Sort. Despite yielding eGFP-Sort, analysis of fractions 3-6 (10% Buffer B) and 9-12 (15% Buffer B) showed the presence of the truncations and other contaminants. In comparison fraction 17 (40% Buffer B) which although contained a high concentration of eGFP-Sort was heavily contaminated. Whilst the observed abundance of the dimer species may arise within the fraction due to the concentration of eGFP-Sort, it likely represents stronger binding of the dimer species as the dimer is seen in fractions 9-12 but not 3-6. Likewise, the high concentration of the truncation species suggests that these products bind strongly. This is to be expected as truncations likely represent the His-tag containing N-terminal regions. Based on their high concentration of eGFP-Sort, fractions 3-12 were chosen to be combined, dialysed and spin concentrated to a stock concentration of 8.86 mg/mL (184 µM). Post enterokinase cleavage of the His-Tag and N-terminal region should remove the contaminants, as the cleaved eGFP-Sort should not bind during another round of Ni-affinity IMAC.

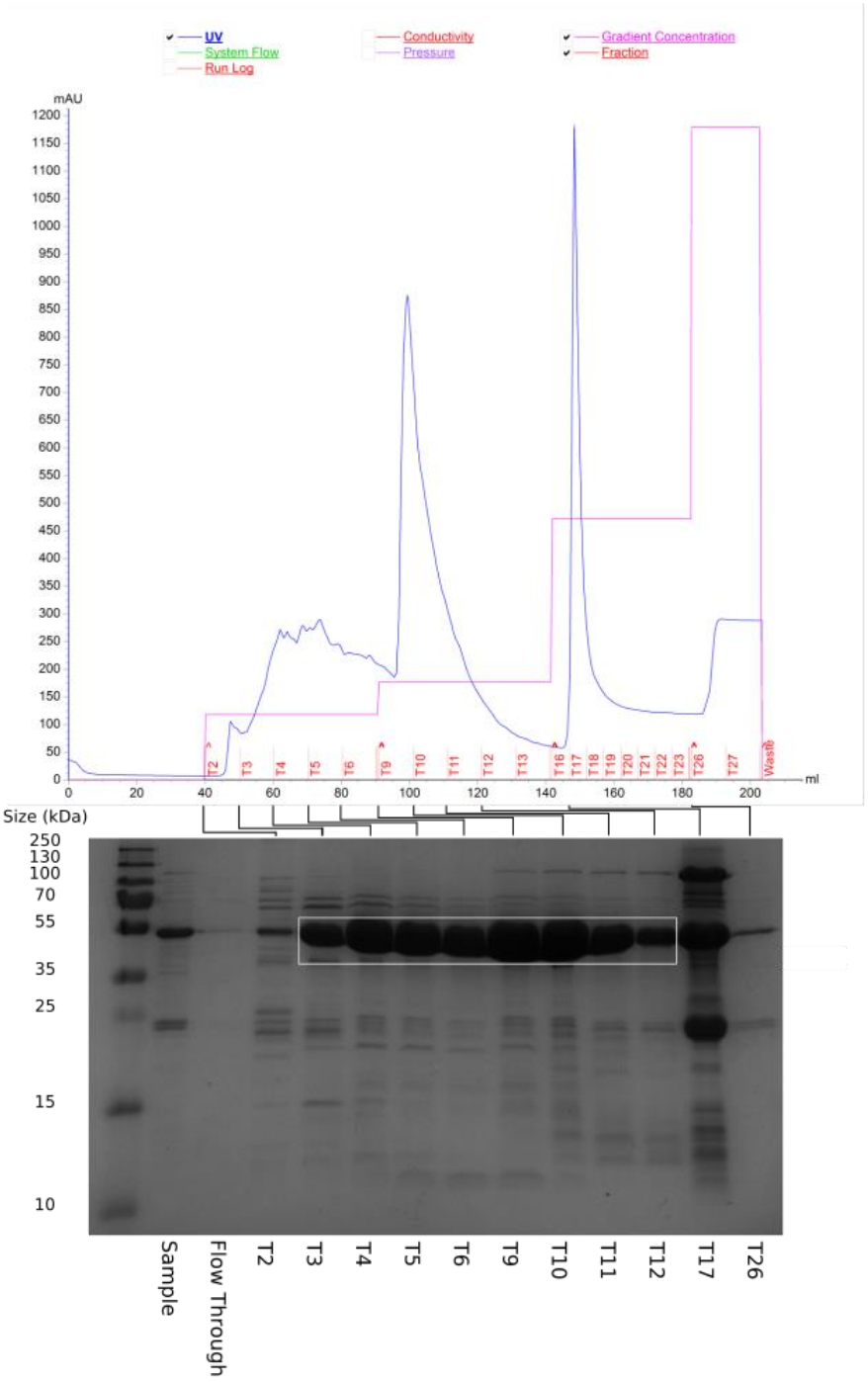


Figure 14. Secondary IMAC purification of eGFP-Sort. The chromatogram displays the UV absorbance of column flow through being collected in 10 mL fractions (red) through the increasing Buffer B concentration gradient (Pink). The SDS PAGE gels show the proteins presence in these fractions, unbound eGFP-Sort (Flow Through) and the original sample. Fractions showing high concentrations of eGFP-Sort (Mw 47.9 kDa) are highlighted.

3.6.3 Test Expression of eGFP-SH3b

eGFP-SH3b expression tests were performed to establish the conditions for overexpression. Like eGFP-Sort (Figure 12), expression was initially investigated at 30 ^{o}C but similarly the protein displayed a high degree of insolubility (See Figure 15a). Unlike eGFP-Sort, lowering the incubation temperature to 20 ^{o}C did not appear to reduce the proportion of insoluble protein. Incubation at 15 ^{o}C did however improve eGFP-SH3b solubility (See Figure 15b). Like eGFP-Sort there does appear to be the presence of an insoluble truncation product between 10 and 15 kDa when expressed at 30 ^{o}C. Again, it is not clear due to warping whether this is also present in the soluble fraction. Interestingly, the uninduced samples in both Figures 12b and 15b display the warped bands observed between 10 and 15 kDa. This suggests that the warped bands seen at this size are artefacts produced by the aggregation of small proteins, rather than the truncation product observed in the insoluble 30 ^{o}C fraction. This would suggest that the higher temperature was causing exhaustion of the expression machinery, resulting in a truncation that because of its composition or folding was highly insoluble.

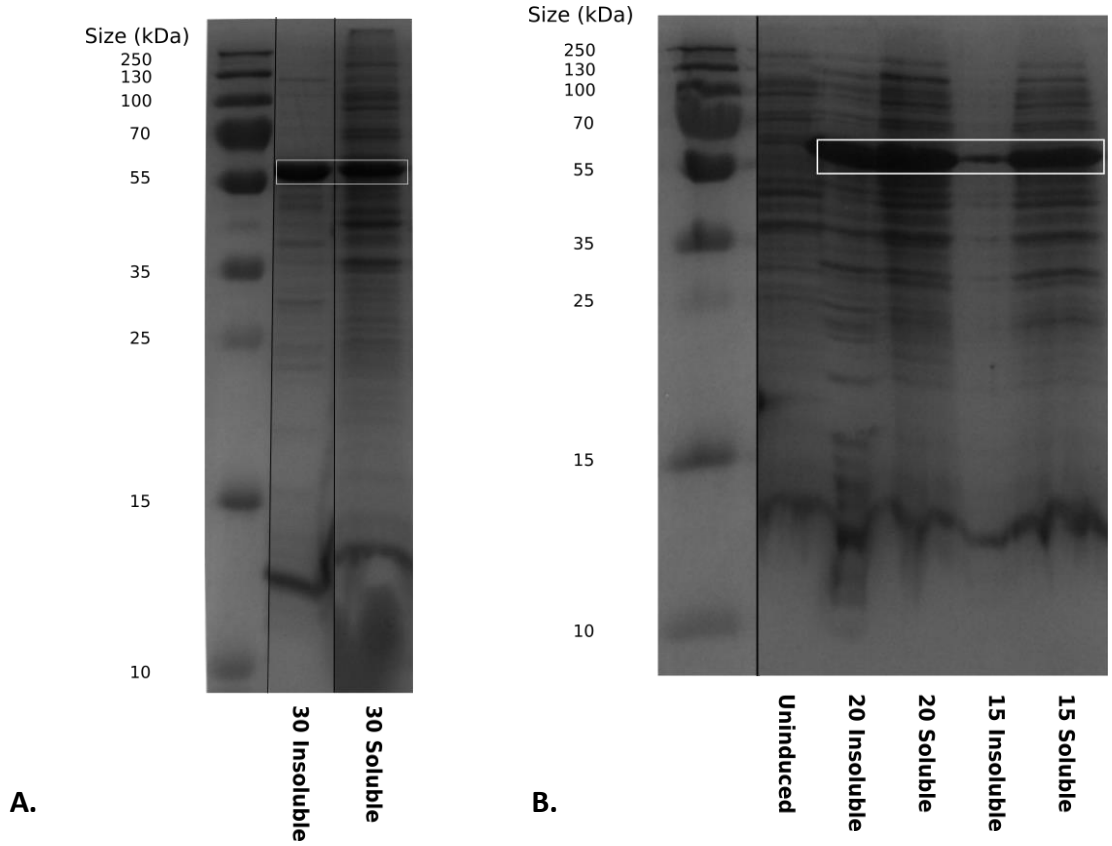


Figure 15: Test expression of eGFP-SH3b. A) Insoluble and Soluble fractions of BL21 (DE3) cells expressing eGFP-SH3b at 30°C for 4 hours. B) Whole cell lysate of uninduced cells with both soluble and insoluble fractions from expression cultures incubated at either 20 or 15 °C. eGFP-SH3b is highlighted by the boxes. Mw of eGFP-SH3b = 55.5 kDa.

3.6.4 Overexpression of eGFP-SH3b

eGFP-SH3b was overexpressed at 15 ^{o}C and purified by one round of Ni-IMAC. A combination of step and gradient changes in Buffer B concentration were used during purification (See Figure 16). Fraction 2 representing the initial 10% step displays several proteins that most likely represent endogenous proteins with weak Ni-binding affinity such as DnaK (70 kDa) and Yoda (22 kDa)[102]. Fractions 7, 8 and 9 show increasing Buffer B to 15 % was optimal for eluting the majority of eGFP-SH3b bound to the column. To remove any other bound eGFP-SH3b a concentration gradient from 15% to 50% was applied. This gradient produced two smaller peaks in absorbance, which were collected as fractions 13 and 14. Examination of 13 and 14 showed that like fractions 7, 8 and 9 they both contained eGFP-SH3b, however, fraction 14 contained two prominent contaminants. These contaminants likely represent similar truncation and dimer species as those observed in the eGFP-Sort purification and can also be seen in the 100% wash fraction 20. The low contaminant containing fractions 7-13 were combined, dialysed, and concentrated using PEG to a concentration of 3.16 mg/mL.

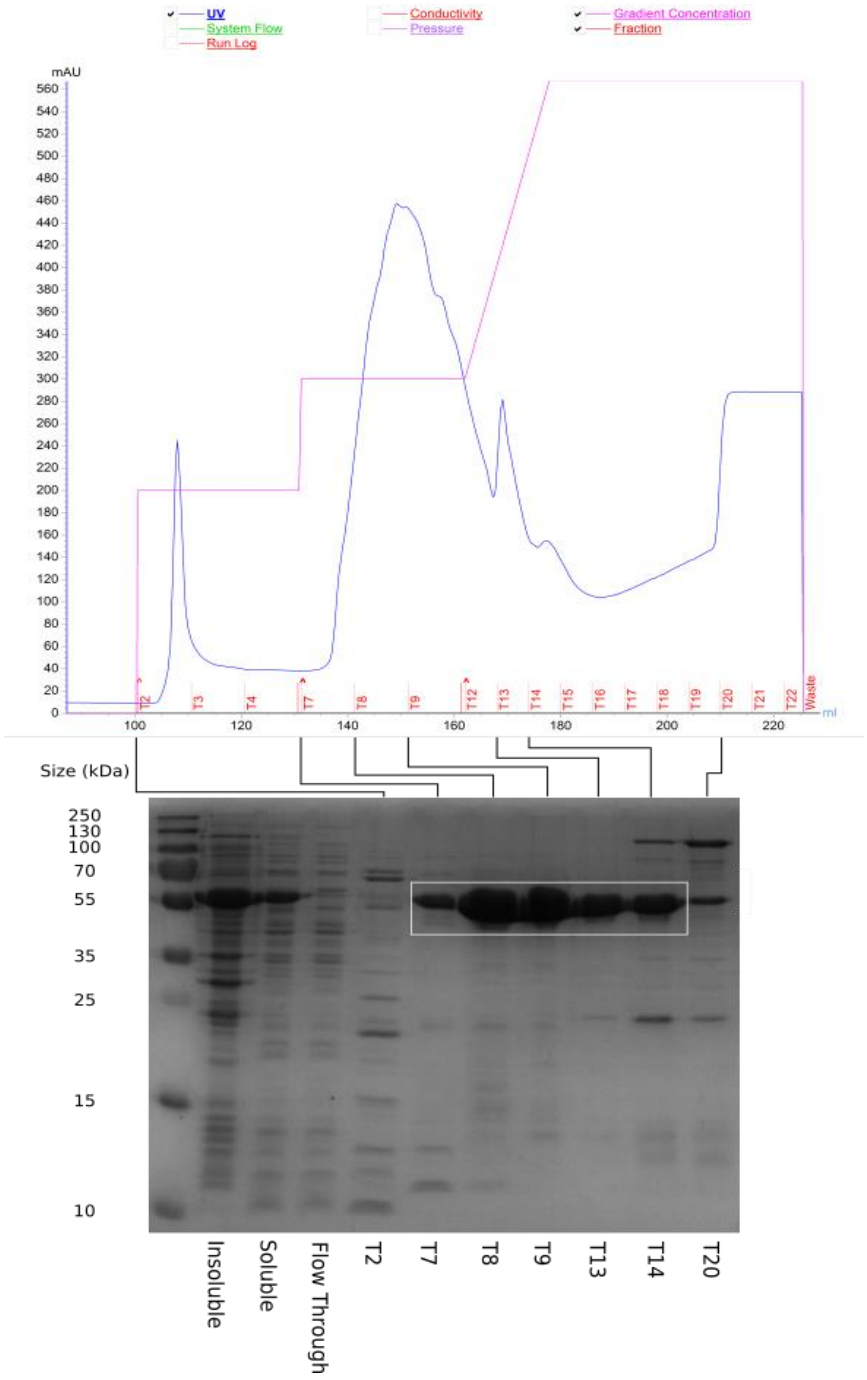


Figure 16: IMAC purification of eGFP-SH3b. The chromatogram displays the UV absorbance of column flow through being collected in 10 mL fractions (red) through the increasing Buffer B concentration gradient (Pink). The SDS PAGE gels show the proteins presence in these fractions, proteins that did not bind during loading (Flow Through) and both insoluble and supernatant fractions following lysis. Fractions showing high concentrations of eGFP-SH3b (Mw 55.5 kDa) are highlighted.

4. Conclusion

This work has developed a library of expression constructs and produced an initial purification of both eGFP-SH3b and eGFP-sort fusion proteins. Which shall be utilised in future work investigating the potential of exploiting the endogenous Sortase A pathway for the targeting of proteins to cell wall of *S. aureus*. As expected, gene synthesis and HiFi assembly streamlined the generation of the construct library. However, in hindsight the selection of a different cloning and / or expression vector may have been preferential, as pET32a is a low copy number plasmid. Making the obtaining of miniprep yields high enough for sequencing and manipulation difficult.

The largest obstacle arose during test expressions. Where the production of truncated protein and insolubility affected the expression of eGFP Sort and LSS fusions. With trial expressions of LSS-Full producing only truncated product; LSS-Sort producing both full length and truncated proteins, and no products for LSS-SH3b. Like the eGFP fusions, this could be arising due to the presence of rare codons causing trans-translation events in which translation is terminated, resulting in a truncated protein[103]. In such events these proteins become tagged for degradation by proteases including the Lon protease[104], which is knocked-out in BL21 (DE3) strains. The absence of which may have attenuated the degradation of truncates resulting in the high abundance of truncated proteins observed. This hypothesis could be tested by the expression of constructs assembled from synthesized catalytic domain coding sequences, as they were codon optimized and as such should not experience truncation.

Where codon usage is probably an issue for LSS and eGFP constructs it would be beneficial to use a Rosetta strain of BL21 (DE3), which carries the pRARE plasmid. This plasmid encodes tRNAs for the rare AGG, AGA, AUA, CUA, CCC, GGA codons, circumventing the need to optimize the codon usages. Additionally, modulating the levels of expression by optimizing the IPTG induction concentration could not only increase protein solubility but may also reduce truncation products. As the rate of translation would be decreased to a point where the available pool of primed tRNAs are not exhausted and translational stalling is avoided.

The next stage of the project should focus on expression of eGFP without a cell wall targeting domain, and to perform cleavage and polishing steps on all three eGFP proteins. These proteins can then be used to determine if the endogenous sortase is able to incorporate exogenous proteins into staphylococcal cell walls. Using confocal microscopy, qualitative confirmation can be made to whether eGFP-Sort localizes to the cell wall of *S. aureus*, whilst florescence spectroscopy can confirm and quantify whether this is due to covalent anchoring. In these experiments the eGFP-SH3b provides a positive control for localization and transient binding, whilst eGFP alone provides a negative control for background signal[76,105]. Subsequently, expression and purification of the catalytic domain fusions would be performed to provide protein with which to perform turbidity reduction assays. Using this assay, the lytic activity of each fusion protein will be determined by measuring the change in liquid *S. aureus* culture density. This will be used to evaluate each fusions anti-staphylococcal activity and to compare the relative contribution of the sort-tag and SH3b domain to activity.

If these experiments show that the sortase pathway is a viable method of targeting the staphylococcal cell wall, then future work could either look to optimize the use of peptidoglycan hydrolase domains or investigate the use of alternative 'warhead' domains. In terms of optimization, this could involve altering the linker length or the sequence of the sorting signal. Whilst conjugation of antimicrobial agents provides an alternative to the use of catalytic domains. Such an approach has already proved successful for silver nanoparticles when conjugated to the SH3b domain of lysostaphin[106]. Whilst photosensitizers have also demonstrated some potential when delivered by phage or antibody[107,108]. An alternative approach to antimicrobial activity could be to promote host immune responses by conjugating antigens to these sort-tags.

5. Bibliography

1 Kluytmans, J., van Belkum, A. & Verbrugh, H. Nasal carriage of *Staphylococcus aureus*: epidemiology, underlying mechanisms, and associated risks. *Clin Microbiol Rev* **10**, 505-520, (1997).

2 Public Health England. Laboratory surveillance of *Staphylococcus aureus* bacteraemia in England and Northern Ireland: 2016. (2017).

3 Chambers, H. F. & DeLeo, F. R. Waves of resistance: *Staphylococcus aureus* in the antibiotic era. *Nature Reviews Microbiology* **7**, 629, (2009).

4 Rayner, C. & Munckhof, W. J. Antibiotics currently used in the treatment of infections caused by *Staphylococcus aureus*. *Internal Medicine Journal* **35**, 3-16, (2005).

5 Joint Formulary Committee. *British National Formulary*. 77 edn, (BMJ Group and Pharmaceutical Press, 2019).

6 Alder, J. The Use of Daptomycin for *Staphylococcus Aureus* Infections in Critical Care Medicine. *Critical Care Clinics* **24**, 349-363, (2008).

7 Marty, F. M. *et al.* Emergence of a Clinical Daptomycin-Resistant *Staphylococcus aureus* Isolate during Treatment of Methicillin-Resistant *Staphylococcus aureus* Bacteremia and Osteomyelitis. *Journal of Clinical Microbiology* **44**, 595-597, (2006).

8 Toh, S. M. *et al.* Acquisition of a natural resistance gene renders a clinical strain of methicillin-resistant *Staphylococcus aureus* resistant to the synthetic antibiotic linezolid. *Molecular Microbiology* **64**, 1506-1514, (2007).

9 Olsen, J. E., Christensen, H. & Aarestrup, F. M. Diversity and evolution of blaZ from *Staphylococcus aureus* and coagulase-negative staphylococci. *The Journal of antimicrobial chemotherapy* **57**, 450-460, (2006).

10 Cafini, F. *et al.* Horizontal gene transmission of the cfr gene to MRSA and Enterococcus: role of *Staphylococcus epidermidis* as a reservoir and alternative pathway for the spread of linezolid resistance. *Journal of Antimicrobial Chemotherapy* **71**, 587-592, (2015).

11 Otsuka, T. *et al.* Macrolide–lincosamide–streptogramin B resistance phenotypes and genotypes among *Staphylococcus aureus* clinical isolates in Japan. *Clinical Microbiology and Infection* **13**, 325-327, (2007).

12 Huang, J. *et al.* Novel Chromosomally Encoded Multidrug Efflux Transporter MdeA in *Staphylococcus aureus*. *Antimicrobial Agents and Chemotherapy* **48**, 909, (2004).

13 World Health Organization. Global priority list of antibiotic-resistant bacteria to guide research, discovery, and development of new antibiotics. 5 (World Health Organization, 2017).

14 Ventola, C. L. The antibiotic resistance crisis: part 1: causes and threats. *Pharmacy and Therapeutics* **40**, 277-283, (2015).

15 Williamson, R., Collatz, E. & Gutmann, L. Mechanisms of action of beta-lactam antibiotics and mechanisms of non-enzymatic resistance. *La Presse médicale* **15**, 2282-2289, (1986).

16 Watanakunakorn, C. Mode of action and in-vitro activity of vancomycin. *Journal of Antimicrobial Chemotherapy* **14**, 7-18, (1984).

17 Tipper, D. J., Strominger, J. L. & Ensign, J. C. Structure of the cell wall of Staphylococcus aureus, strain Copenhagen. VII. Mode of action of the bacteriolytic peptidase from

Myxobacter and the isolation of intact cell wall polysaccharides. *Biochemistry* **6**, 906-920, (1967).
18 Ward, J. B. The chain length of the glycans in bacterial cell walls. *The Biochemical journal* **133**, 395-398, (1973).
19 Boneca, I. G., Huang, Z.-H., Gage, D. A. & Tomasz, A. Characterization of Staphylococcus aureus Cell Wall Glycan Strands, Evidence for a New β-N-Acetylglucosaminidase Activity. *Journal of Biological Chemistry* **275**, 9910-9918, (2000).
20 Yamada, S. *et al.* An autolysin ring associated with cell separation of Staphylococcus aureus. *Journal of bacteriology* **178**, 1565-1571, (1996).
21 Höltje, J. V. Growth of the stress-bearing and shape-maintaining murein sacculus of Escherichia coli. *Microbiology and Molecular Biology Reviews* **62**, 181-203, (1998).
22 Bose, J. L., Lehman, M. K., Fey, P. D. & Bayles, K. W. Contribution of the *Staphylococcus aureus* Atl AM and GL Murein Hydrolase Activities in Cell Division, Autolysis, and Biofilm Formation. *PLOS ONE* **7**, https://doi.org/10.1371/journal.pone.0042244, (2012).
23 Recsei, P. A., Gruss, A. D. & Novick, R. P. Cloning, sequence, and expression of the lysostaphin gene from *Staphylococcus simulans*. *Proceedings of the National Academy of Sciences* **84**, 1127, (1987).
24 Wang, S. *et al.* First report of a novel plant lysozyme with both antifungal and antibacterial activities. *Biochemical and Biophysical Research Communications* **327**, 820-827, (2005).
25 Takác, M. & Bläsi, U. Phage P68 virion-associated protein 17 displays activity against clinical isolates of Staphylococcus aureus. *Antimicrobial agents and chemotherapy* **49**, 2934-2940, (2005).
26 Rodríguez-Rubio, L. *et al.* The Phage Lytic Proteins from the *Staphylococcus aureus* Bacteriophage vB_SauS-phiIPLA88 Display Multiple Active Catalytic Domains and Do Not Trigger Staphylococcal Resistance. *PLOS ONE* **8**, https://doi.org/10.1371/journal.pone.0064671, (2013).
27 Evrard, C., Fastrez, J. & Declercq, J. P. Crystal structure of the lysozyme from bacteriophage lambda and its relationship with V and C-type lysozymes11. *Journal of Molecular Biology* **276**, 151-164, (1998).
28 Oliveira, H. *et al.* Structural and Enzymatic Characterization of ABgp46, a Novel Phage Endolysin with Broad Anti-Gram-Negative Bacterial Activity. *Frontiers in microbiology* **7**, 208-208, (2016).
29 Becker, S. C. *et al.* LysK CHAP endopeptidase domain is required for lysis of live staphylococcal cells. *FEMS Microbiology Letters* **294**, 52-60, (2009).
30 Rodríguez-Rubio, L., Martínez, B., Rodríguez, A., Donovan, D. M. & García, P. Enhanced Staphylolytic Activity of the Staphylococcus aureus Bacteriophage vB_SauS-phiIPLA88 HydH5 Virion-Associated Peptidoglycan Hydrolase: Fusions, Deletions, and Synergy with LysH5. *Applied and Environmental Microbiology* **78**, 2241-2248, (2012).
31 Sabala, I., Jonsson, I.-M., Tarkowski, A. & Bochtler, M. Anti-staphylococcal activities of lysostaphin and LytM catalytic domain. *BMC microbiology* **12**, 97-97, (2012).
32 Büttner, F. M., Zoll, S., Nega, M., Götz, F. & Stehle, T. Structure-Function Analysis of *Staphylococcus aureus* Amidase Reveals the Determinants of Peptidoglycan Recognition and Cleavage. *Journal of Biological Chemistry* **289**, 11083-11094, (2014).
33 Becker, S. C. *et al.* Lytic activity of the staphylolytic Twort phage endolysin CHAP domain is enhanced by the SH3b cell wall binding domain. *FEMS Microbiol Lett* **362**, 1-8, (2015).

34 Blackburn, N. T. & Clarke, A. J. Identification of Four Families of Peptidoglycan Lytic Transglycosylases. *Journal of Molecular Evolution* **52**, 78-84, (2001).
35 Gargis, S. R. *et al.* Inhibition of the Activity of Both Domains of Lysostaphin through Peptidoglycan Modification by the Lysostaphin Immunity Protein. *Appl Environ Microbiol* **76**, 6944-6946, (2010).
36 Sabala, I. *et al.* Crystal structure of the antimicrobial peptidase lysostaphin from *Staphylococcus simulans*. *The FEBS Journal* **281**, 4112-4122, (2014).
37 Warfield, R. *et al.* Internally quenched peptides for the study of lysostaphin: an antimicrobial protease that kills *Staphylococcus aureus*. *Organic & Biomolecular Chemistry* **4**, 3626-3638, (2006).
38 Horgan, M. *et al.* Phage Lysin LysK Can Be Truncated to Its CHAP Domain and Retain Lytic Activity against Live Antibiotic-Resistant Staphylococci. *Applied and Environmental Microbiology* **75**, 872-874, (2009).
39 Rodríguez, L. *et al.* Lytic activity of the virion-associated peptidoglycan hydrolase HydH5 of *Staphylococcus aureus* bacteriophage vB_SauS-phiIPLA88. *BMC Microbiology* **11**, 138, (2011).
40 Heilmann, C., Hussain, M., Peters, G. & Götz, F. Evidence for autolysin-mediated primary attachment of *Staphylococcus epidermidis* to a polystyrene surface. *Molecular Microbiology* **24**, 1013-1024, (1997).
41 Biswas, R. *et al.* Activity of the major staphylococcal autolysin Atl. *FEMS Microbiol Lett* **259**, 260-268, (2006).
42 Schlag, M. *et al.* Role of staphylococcal wall teichoic acid in targeting the major autolysin Atl. *Mol Microbiol* **75**, 864-873, (2010).
43 Gorski, A. *et al.* Phage as a modulator of immune responses: practical implications for phage therapy. *Adv Virus Res* **83**, 41-71, (2012).
44 Fauconnier, A. Regulating phage therapy: The biological master file concept could help to overcome regulatory challenge of personalized medicines. *EMBO reports* **18**, 198-200, (2017).
45 Forde, A. & Hill, C. Phages of life - the path to pharma. *Br J Pharmacol* **175**, 412-418, (2018).
46 Loeffler, J. M., Nelson, D. & Fischetti, V. A. Rapid killing of *Streptococcus pneumoniae* with a bacteriophage cell wall hydrolase. *Science* **294**, 2170-2172, (2001).
47 Nelson, D., Loomis, L. & Fischetti, V. A. Prevention and elimination of upper respiratory colonization of mice by group A streptococci by using a bacteriophage lytic enzyme. *Proceedings of the National Academy of Sciences of the United States of America* **98**, 4107-4112, (2001).
48 Schuch, R., Nelson, D. & Fischetti, V. A. A bacteriolytic agent that detects and kills Bacillus anthracis. *Nature* **418**, 884-889, (2002).
49 Schmelcher, M. *et al.* Evolutionarily distinct bacteriophage endolysins featuring conserved peptidoglycan cleavage sites protect mice from MRSA infection. *Journal of Antimicrobial Chemotherapy* **70**, 1453-1465, (2015).
50 Daniel, A. *et al.* Synergism between a novel chimeric lysin and oxacillin protects against infection by methicillin-resistant Staphylococcus aureus. *Antimicrobial agents and chemotherapy* **54**, 1603-1612, (2010).
51 Jun, S. Y. *et al.* Pharmacokinetics and Tolerance of the Phage Endolysin-Based Candidate Drug SAL200 after a Single Intravenous Administration among Healthy Volunteers. *Antimicrob Agents Chemother* **61**, (2017).

52 Schuch, R., Khan, B. K., Raz, A., Rotolo, J. A. & Wittekind, M. Bacteriophage Lysin CF-301, a Potent Antistaphylococcal Biofilm Agent. *Antimicrobial Agents and Chemotherapy* **61**, e02666-02616, (2017).
53 Paul, V. D. *et al.* A novel bacteriophage Tail-Associated Muralytic Enzyme (TAME) from Phage K and its development into a potent antistaphylococcal protein. *BMC Microbiol* **11**, 226, (2011).
54 Schmelcher, M., Tchang, V. S. & Loessner, M. J. Domain shuffling and module engineering of Listeria phage endolysins for enhanced lytic activity and binding affinity. *Microbial Biotechnology* **4**, 651-662, (2011).
55 ClinicalTrials.gov. *Safety & Efficacy of an Antibacterial Protein Molecule Applied Topically to the Nostrils of Volunteers and Patients*, <https://ClinicalTrials.gov/show/NCT01746654> (2019).
56 Sundarrajan, S. *et al.* Bacteriophage-derived CHAP domain protein, P128, kills Staphylococcus cells by cleaving interpeptide cross-bridge of peptidoglycan. *Microbiology (Reading, England)* **160**, 2157-2169, (2014).
57 Totté, J. E. E., van Doorn, M. B. & Pasmans, S. G. M. A. Successful Treatment of Chronic *Staphylococcus aureus*-Related Dermatoses with the Topical Endolysin Staphefekt SA.100: A Report of 3 Cases. *Case Rep Dermatol* **9**, 19-25, (2017).
58 Loessner, M. J. & Eichenseher, F. A Novel Endolysin Polypeptide. (2017).
59 Climo, M. W., Patron, R. L., Goldstein, B. P. & Archer, G. L. Lysostaphin treatment of experimental methicillin-resistant *Staphylococcus aureus* aortic valve endocarditis. *Antimicrob Agents Chemother* **42**, 1355-1360, (1998).
60 Patron, R. L., Climo, M. W., Goldstein, B. P. & Archer, G. L. Lysostaphin treatment of experimental aortic valve endocarditis caused by a *Staphylococcus aureus* isolate with reduced susceptibility to vancomycin. *Antimicrob Agents Chemother* **43**, 1754-1755, (1999).
61 Mohamed, M. F., Hamed, M. I., Panitch, A. & Seleem, M. N. Targeting methicillin-resistant *Staphylococcus aureus* with short salt-resistant synthetic peptides. *Antimicrob Agents Chemother* **58**, 4113-4122, (2014).
62 Johnson, C. T. *et al.* Hydrogel delivery of lysostaphin eliminates orthopedic implant infection by *Staphylococcus aureus* and supports fracture healing. *Proceedings of the National Academy of Sciences* **115**, E4960-E4969, (2018).
63 Kokai-Kun, J. F., Chanturiya, T. & Mond, J. J. Lysostaphin as a treatment for systemic Staphylococcus aureus infection in a mouse model. *The Journal of antimicrobial chemotherapy* **60**, 1051-1059, (2007).
64 Wu, J. A., Kusuma, C., Mond, J. J. & Kokai-Kun, J. F. Lysostaphin Disrupts *Staphylococcus aureus* and *Staphylococcus epidermidis* Biofilms on Artificial Surfaces. *Antimicrobial Agents and Chemotherapy* **47**, 3407-3414, (2003).
65 Walencka, E., Sadowska, B., Rozalska, S., Hryniewicz, W. & Rozalska, B. Lysostaphin as a potential therapeutic agent for staphylococcal biofilm eradication. *Polish journal of microbiology* **54**, 191-200, (2005).
66 Gu, J. *et al.* LysGH15B, the SH3b Domain of Staphylococcal Phage Endolysin LysGH15, Retains High Affinity to Staphylococci. *Current Microbiology* **63**, 538, (2011).
67 Tossavainen, H. *et al.* Structural and Functional Insights Into Lysostaphin-Substrate Interaction. *Frontiers in molecular biosciences* **5**, 60-60, (2018).
68 Mitkowski, P. *et al.* Structural bases of peptidoglycan recognition by lysostaphin SH3b domain. *Scientific Reports* **9**, 5965, (2019).

69 Donovan, D. M. *et al.* Peptidoglycan hydrolase fusions maintain their parental specificities. *Appl Environ Microbiol* **72**, 2988-2996, (2006).
70 Idelevich, E. A. *et al.* In Vitro Activity against *Staphylococcus aureus* of a Novel Antimicrobial Agent, PRF-119, a Recombinant Chimeric Bacteriophage Endolysin. *Antimicrobial Agents and Chemotherapy*, 10.1128/AAC.00217-00211, (2011).
71 Schmelcher, M., Powell, A. M., Becker, S. C., Camp, M. J. & Donovan, D. M. Chimeric Phage Lysins Act Synergistically with Lysostaphin To Kill Mastitis-Causing *Staphylococcus aureus* in Murine Mammary Glands. *Applied and environmental microbiology* **78**, 2297-2305, (2012).
72 Jagielska, E., Chojnacka, O. & Sabała, I. LytM Fusion with SH3b-Like Domain Expands Its Activity to Physiological Conditions. *Microb Drug Resist* **22**, 461-469, (2016).
73 Tschierske, M., Ehlert, K., Stranden, A. M. & Berger-Bachi, B. Lif, the lysostaphin immunity factor, complements FemB in staphylococcal peptidoglycan interpeptide bridge formation. *FEMS Microbiol Lett* **153**, 261-264, (1997).
74 Ehlert, K., Schroder, W. & Labischinski, H. Specificities of FemA and FemB for different glycine residues: FemB cannot substitute for FemA in staphylococcal peptidoglycan pentaglycine side chain formation. *J Bacteriol* **179**, 7573-7576, (1997).
75 Climo, M. W., Ehlert, K. & Archer, G. L. Mechanism and suppression of lysostaphin resistance in oxacillin-resistant *Staphylococcus aureus*. *Antimicrob Agents Chemother* **45**, 1431-1437, (2001).
76 Gründling, A. & Schneewind, O. Cross-Linked Peptidoglycan Mediates Lysostaphin Binding to the Cell Wall Envelope of *Staphylococcus aureus*. *Journal of Bacteriology* **188**, 2463, (2006).
77 Strandén, A., M, K, E., Labischinski, H. & Berger-Bächi, B. Cell Wall Monoglycine Cross-Bridges and Methicillin Hypersusceptibility in a femAB Null Mutant of Methicillin-Resistant *Staphylococcus aureus. Journal of Bacteriology* **179**, 9-16, (1997).
78 Kusuma, C., Jadanova, A., Chanturiya, T. & Kokai-Kun, J. F. Lysostaphin-Resistant Variants of Staphylococcus aureus Demonstrate Reduced Fitness In Vitro and In Vivo. *Antimicrobial Agents and Chemotherapy* **51**, 475-482, (2007).
79 Ehlert, K., Tschierske, M., Mori, C., Schröder, W. & Berger-Bächi, B. in *Journal of Bacteriology* Vol. 182 2635-2638 (2000).
80 Becker, S. C., Foster-Frey, J., Stodola, A. J., Anacker, D. & Donovan, D. M. Differentially conserved staphylococcal SH3b_5 cell wall binding domains confer increased staphylolytic and streptolytic activity to a streptococcal prophage endolysin domain. *Gene* **443**, 32-41, (2009).
81 Zoll, S. *et al.* Ligand-Binding Properties and Conformational Dynamics of Autolysin Repeat Domains in Staphylococcal Cell Wall Recognition. *Journal of Bacteriology* **194**, 3789-3802, (2012).
82 Chang, Y. & Ryu, S. Characterization of a novel cell wall binding domain-containing *Staphylococcus aureus* endolysin LysSA97. *Appl Microbiol Biotechnol* **101**, 147-158, (2017).
83 Mazmanian, S. K., Liu, G., Jensen, E. R., Lenoy, E. & Schneewind, O. *Staphylococcus aureus* sortase mutants defective in the display of surface proteins and in the pathogenesis of animal infections. *Proceedings of the National Academy of Sciences* **97**, 5510, (2000).
84 Suree, N. *et al.* The structure of the *Staphylococcus aureus* sortase-substrate complex reveals how the universally conserved LPXTG sorting signal is recognized. *The Journal of biological chemistry* **284**, 24465-24477, (2009).

85 Frankel, B. A., Bentley, M., Kruger, R. G. & McCafferty, D. G. Vinyl Sulfones: Inhibitors of SrtA, a Transpeptidase Required for Cell Wall Protein Anchoring and Virulence in *Staphylococcus aureus*. *Journal of the American Chemical Society* **126**, 3404-3405, (2004).
86 Wang, J. *et al.* Astilbin Inhibits the Activity of Sortase A from Streptococcus mutans. *Molecules* **24**, 456, (2019).
87 Zhang, J. *et al.* Antiinfective therapy with a small molecule inhibitor of *Staphylococcus aureus* sortase. *Proc Natl Acad Sci USA* **111**, 13517-13522, (2014).
88 Wang, J. *et al.* Oligopeptide Targeting Sortase A as Potential Anti-infective Therapy for *Staphylococcus aureus*. *Frontiers in Microbiology* **9**, 10.3389/fmicb.2018.00245, (2018).
89 Mazmanian, S. K., Liu, G., Ton-That, H. & Schneewind, O. *Staphylococcus aureus* sortase, an enzyme that anchors surface proteins to the cell wall. *Science* **285**, 760-763, (1999).
90 Navarre, W. W. & Schneewind, O. Proteolytic cleavage and cell wall anchoring at the LPXTG motif of surface proteins in Gram-positive bacteria. *Molecular Microbiology* **14**, 115-121, (1994).
91 Perry, A. M., Ton-That, H., Mazmanian, S. K. & Schneewind, O. Anchoring of Surface Proteins to the Cell Wall of *Staphylococcus aureus*. *Journal of Biological Chemistry* **277**, 16241-16248, (2002).
92 Popp, M. W., Antos, J. M., Grotenbreg, G. M., Spooner, E. & Ploegh, H. L. Sortagging: a versatile method for protein labeling. *Nature Chemical Biology* **3**, 707, (2007).
93 Pishesha, N., Ingram, J. R. & Ploegh, H. L. Sortase A: A Model for Transpeptidation and Its Biological Applications. *Annual Review of Cell and Developmental Biology* **34**, 163-188, (2018).
94 Goodyear, C. S. & Silverman, G. J. Death by a B cell superantigen: In vivo VH-targeted apoptotic supraclonal B cell deletion by a Staphylococcal Toxin. *The Journal of experimental medicine* **197**, 1125-1139, (2003).
95 Falugi, F., Kim, H. K., Missiakas, D. M. & Schneewind, O. Role of Protein A in the Evasion of Host Adaptive Immune Responses by *Staphylococcus aureus*. *mBio* **4**, e00575-00513, (2013).
96 Schneewind, O., Mihaylova-Petkov, D. & Model, P. Cell wall sorting signals in surface proteins of gram-positive bacteria. *The EMBO journal* **12**, 4803-4811, (1993).
97 Hansenová Maňásková, S. *et al.* Synthetic LPETG-Containing Peptide Incorporation in the *Staphylococcus aureus* Cell-Wall in a Sortase A- and Growth Phase-Dependent Manner. *PLOS ONE* **9**, https://doi.org/10.1371/journal.pone.0089260, (2014).
98 Hansenová Maňásková, S. *et al. Staphylococcus aureus* Sortase A-Mediated Incorporation of Peptides: Effect of Peptide Modification on Incorporation. *PLOS ONE* **11**, https://doi.org/10.1371/journal.pone.0147401, (2016).
99 Sigma-Aldrich. *TB122VM pET-32a-c(+) Vector Map*, <http://www.merckmillipore.com/GB/en/product/pET-32a+-DNA-Novagen,EMD_BIO-69015#anchor_BRO> (2019).
100 Sambrook, J., Fritsch, E. F. & Maniatis, T. *Molecular cloning: a laboratory manual.*, (Cold Spring Harbor Laboratory Press, 1989).
101 Gasteiger, E. *et al.* in *The Proteomics Protocols Handbook* (ed John M Walker) 571-607 (Humana Press, 2019).
102 Bolanos-Garcia, V. M. & Davies, O. R. Structural analysis and classification of native proteins from E. coli commonly co-purified by immobilised metal affinity chromatography. *Biochimica et biophysica acta* **1760**, 1304-1313, (2006).

103 Roche, E. D. & Sauer, R. T. SsrA-mediated peptide tagging caused by rare codons and tRNA scarcity. *The EMBO Journal* **18**, 4579-4589, (1919).
104 Choy, J. S., Aung, L. L. & Karzai, A. W. Lon Protease Degrades Transfer-Messenger RNA-Tagged Proteins. *Journal of Bacteriology* **189**, 6564-6567, (2007).
105 Briers, Y. *et al.* Muralytic activity and modular structure of the endolysins of Pseudomonas aeruginosa bacteriophages ϕKZ and EL. *Molecular Microbiology* **65**, 1334-1344, (2007).
106 Kim, D. *et al.* Selective Killing of Pathogenic Bacteria by Antimicrobial Silver Nanoparticle—Cell Wall Binding Domain Conjugates. **10**, 13317-13324, (2018).
107 Embleton, M. L., Nair, S. P., Cookson, B. D. & Wilson, M. Selective lethal photosensitization of methicillin-resistant *Staphylococcus aureus* using an IgG–tin (IV) chlorin e6 conjugate. *Journal of Antimicrobial Chemotherapy* **50**, 857-864, (2002).
108 Embleton, M. L. *et al.* Development of a novel targeting system for lethal photosensitization of antibiotic-resistant strains of *Staphylococcus aureus*. *Antimicrob Agents Chemother* **49**, 3690-3696, (2005).